ERICE PREPRINT SERIES
Gu 8402
«ETTORE MAJORANA» CENTRE FOR SCIENTIFIC CULTURE

EMCSC/93-06
10 December 1993

MONTE CARLO SIMULATIONS FOR LEADING PROTON PRODUCTION IN DEEP INELASTIC SCATTERING

A. V. Anisovich[3,9,11], G. Anzivino[4], F. Arzarello[2], G. Bari[2], M. Basile[2,7], L. Bellagamba[2], D. Boscherini[2], G. Bruni[2], P. Bruni[2], G. Cara Romeo[2], M. Chiarini[2,11], L. Cifarelli[2,8], F. Cindolo[2], F. Ciralli[2], A. Contin[1,2], M. Dardo[5,10], S. D'Auria[2], C. Del Papa[2,7], S. De Pasquale[4], F. Frasconi[2], P. Giusti[2], G. Iacobucci[2], G. Maccarrone[4], A. Margotti[2], T. Massam[2], R. Nania[2], S. Qian[2,11], G. Sartorelli[2,7], Yu. M. Shabelski[3,9,11], S. Yu. Sivoklokov[3,6,11], M. A. Stepanov[3,9,11], R. Timellini[2,11], L. Votano[4] and A. Zichichi[1,2]

1) CERN, Geneva, Switzerland
2) INFN, Bologna, Italy
3) INFN, Eloisatron Project, Erice, Italy
4) INFN, LNF, Frascati, Italy
5) INFN, Torino, Italy
6) INP, Moscow State University, Moscow, Russia
7) Physics Department, University of Bologna, Italy
8) Physics Department, University of Pisa, Italy
9) PNPI, Gatchina, St. Petersburg, Russia
10) II Faculty of Science, University of Torino, Alessandria, Italy
11) World Laboratory, Lausanne, Switzerland

Abstract

Predictions for "leading" proton production in Deep Inelastic Scattering at HERA energies are presented in the framework of different Monte Carlo event generators, i.e. LEPTO, HERWIG and PYTHIA, in terms of Feynman-x and transverse momentum distributions. In order to get a comprehensive picture of the various possibilities, different structure functions, different Q^2-values, different reference frames and different types of events (minimum bias events and events with charm and beauty, separately) are considered.

(Submitted to Il Nuovo Cimento)

EMCSC - Via Guarnotta 26 - 91016 Erice - Italy - Tel. (923) 869133 - Fax. (923) 869226

1. INTRODUCTION

The Leading Proton Spectrometer (LPS) of the ZEUS detector [1] at HERA is an essential tool to continue, in ep Deep Inelastic Scattering (DIS) at high energies, the study of the "leading effect", discovered and first studied at ISR [2-27].

In the present paper we consider the predicted x_F (Feynman-x) and p_T^2-distributions of secondary protons as obtained with three different Monte Carlo event generators: LEPTO (version 6.1) [28], HERWIG (version 5.5) [29] and PYTHIA (version 5.6) [30]. There is a significant difference between these event generators, in particular as far as hadronization is concerned. LEPTO and PYTHIA are both based on the ideas of the Lund String Model, but they are differently structured at the stage of hard processes. LEPTO allows one to consider the DIS process as a function of Q^2 and separately in the ep frame (the real laboratory frame) and in the $\gamma^* p$ frame (a more physical one), where γ^* is the exchanged neutral vector-particle. In PYTHIA the so-called Q^2-parameter is not directly related to the four-momentum transfer of DIS in terms of kinematical variables. It represents the effective hardness of the interaction and provides the structure function scale. HERWIG contains the real Q^2-dependence of DIS processes (as LEPTO), but it is based on different physical ideas, being the Monte Carlo version of a particular Cluster Model.

A detailed comparison of the results from these three generators is presented herein. The agreement among the various predictions can illustrate today's generally accepted view on high-energy neutral-current DIS phenomena. Any disagreement can reflect the real difference in the physical pictures described by the three models and therefore suggest interesting experimental tests.

2. FEYNMAN-x DISTRIBUTION OF SECONDARY PROTONS IN DIS

Let us first consider the Feynman-x (x_F) distribution of secondary protons produced in ep collisions at HERA energy ($\sqrt{s} = 314$ GeV). We use the invariant inclusive cross-section[1)] $x_E/\sigma_{ev} \cdot d\sigma/dx_F$, where $x_E = 2E/\sqrt{s}$, $x_F = 2p_L/\sqrt{s}$ (E and p_L being the proton energy and longitudinal momentum, respectively) and σ_{ev} is the total inelastic cross-section, for each class of events considered. In fig. 1a we present the predictions of LEPTO, HERWIG and PYTHIA in the ep centre-of-mass frame for all DIS events. Here and in the following, unless differently specified, LEPTO and HERWIG events are generated at $Q^2 \geq 4$ GeV^2. Notice that 4 GeV^2 is the minimum Q^2-value allowed in LEPTO and also the minimum scale value usable for most of structure function parametrizations. In PYTHIA we use the default Q^2-parameter setting: this corresponds to an effective Q^2-scale ≥ 4 GeV^2 and to a distribution of DIS Q^2-values with $< Q^2 > \sim 2$ GeV^2, where roughly 1/2 of the events have $Q^2 < 1$ GeV^2. A well-defined "leading effect" appears in fig. 1a, since most of the protons are produced at positive x_F-values (i.e. in the direction of the incident proton). The LEPTO and PYTHIA distributions are overlapped and show a plateau in the $x_F > 0$ region, centred around $x_F \sim 0.5$ (as in the case of proton-proton collisions, in each

1) For this cross-section, Feynman scaling should be approximately valid.

x_F-hemisphere [31]). It should be pointed out that LEPTO predictions fit reasonably well the x_F-distributions of protons and antiprotons measured in μp DIS at lower energy [32]. The HERWIG distribution has a narrower plateau, centred around $x_F \sim 0.35$ and rapidly decreasing at relatively high x_F, thus showing a less pronounced "leading effect". In fig. 1a the EHLQ1 [33] set of parton structure functions was used. To check the influence of structure functions, in fig. 1b we present the same distributions obtained with set MT (S-DIS) [34]: although the shapes of the distributions slightly change, the difference between fig. 1a and fig. 1b is not significant and in the following we will always use set EHLQ1. This set is rather "old", however it seems to be more adequate in the case of PYTHIA calculations when these are compared with low-energy data on charm and beauty production in pp collisions [35]. In fig. 1c we show the same spectrum as in fig. 1a once the contribution of "non-leading" protons, i.e. those protons which are pair-produced in the central region together with antiprotons, has been subtracted. To do so we actually subtract from the inclusive x_F-spectrum relative to all protons the corresponding spectrum relative to all antiprotons. The proton spectrum of fig. 1a is practically unaffected by this subtraction in the positive x_F-hemisphere, say at $x_F > 0.1$ (fig. 1c), and keeps its relevant figures, in particular in the forward region at $x_F > 0.5$. In the following we will always consider inclusive distributions, relative to all secondary protons. The same distributions as in fig. 1a are presented in terms of $1/\sigma_{ev} \cdot d\sigma/dx_F$ in fig. 1d where the "non-leading" proton contribution clearly shows up.

Let us now consider the Q^2-dependence of the proton x_F-distribution. As already mentioned, the calculations at different Q^2-values, with Q^2 directly connected with the incident and scattered electron kinematical variables, can only be performed with LEPTO and HERWIG. These are shown in figs. 2a and 2b, respectively, at three different Q^2-values: 7, 100 and 1000 GeV^2. In both cases, the distributions are shifted towards smaller x_F as Q^2 increases: in fact the central production (at $x_F < 0.1$) increases, while the very forward production in the positive x_F-region decreases, i.e. the "leading effect" decreases. In LEPTO this shift is more significant than in HERWIG. The same x_F-distributions obtained with PYTHIA at different Q^2 are presented in fig. 2c. Here the nominal values of Q^2 (7, 100 and 1000 GeV^2) actually correspond to the selection of the previously mentioned Q^2-parameter in the following intervals: $4 \div 10$, $80 \div 120$ and $800 \div 1200$ GeV^2. There is no significant difference between PYTHIA and LEPTO predictions.

The reason for the shift is rather simple. The main contribution to the DIS cross-section at small x_B (Bjorken-x) comes from the γ^* interaction with a sea quark (or antiquark) produced via gluon cascade. When x_B increases, the γ^* interacts with a valence quark of the initial proton with higher probability, so the average number of spectator valence quarks which can recombine into a "leading" proton decreases.

It is also interesting to study the behaviour of secondary protons in DIS events when heavy flavours ($c\bar{c}$ and $b\bar{b}$) are produced. The results with LEPTO, HERWIG and PYTHIA are presented in figs. 3a and 3b, for charm and beauty, respectively. When comparing them with those in fig. 1a, it appears that in both HERWIG and PYTHIA the "leading" proton production at high positive x_F is only slightly affected by the presence of heavy flavours, while it is clearly reduced in LEPTO. The overall effect of heavy flavour production can be better visualized when considering the average x_F of secondary protons, as reported in table 1 for the three event generators considered herein. According to LEPTO, the proton $< x_F >$ decreases by 35% in $c\bar{c}$ events with respect to all (i.e. minimum bias) DIS events. This shift is only 11% in PYTHIA and 6% in HERWIG. When going from $c\bar{c}$ to $b\bar{b}$ events, $< x_F >$ slightly decreases (by only a few %, within the statistical errors) in any of the three event generators, thus showing a weak dependence on the heavy quark mass. Notice that, contrary to fig. 1a, in figs. 3a and 3b the LEPTO and HERWIG predictions are closer and significantly differ from the PYTHIA ones.

In ep interactions, if the main contribution to heavy flavour production is given by the photon-gluon fusion subprocess $\gamma^* g \rightarrow Q\overline{Q}$, $Q\overline{Q}$ ($c\bar{c}$ or $b\bar{b}$) pairs are predominantly produced in the central (or photon fragmentation) region[2)]. And these are mostly meson pairs which hardly decay into protons (and antiprotons). A reduced "leading" proton production in the presence of heavy flavours, as observed in particular with LEPTO, indicates a change in the recombination mechanism of spectator valence quarks with respect to all DIS events, which is likely related to the higher values of Q^2 involved when the γ^* interacts with a heavier sea quark or antiquark. In fact with LEPTO one obtains $< Q^2 > = 27$, 40 and 77 GeV^2 in all, $c\bar{c}$ and $b\bar{b}$ events containing at least one proton, respectively. The influence of heavy flavour production on the proton x_F-distribution also appears when simulating pp interactions. Moreover, the energy level and the choice of structure functions seem to play a role in this respect, as discussed elsewhere [36].

If $< Q^2 >$ increases when going from minimum bias to heavy-flavoured events, it is also instructive to check whether the Q^2-dependence of the proton x_F-distribution is different for these two classes of events. In fig. 4 we show for instance the proton x_F-distribution in events with charm, obtained with LEPTO at $Q^2 = 7$, 100 and 1000 GeV^2 as in fig. 2a for all DIS events. Contrary to fig. 2a, in fig. 4 there is no clear effect of Q^2 on the production of "leading" protons at high x_F.

This fact gives an additional argument to our previous explanation of the shift observed in fig. 2a: for charm production, when the $\gamma^* g$ fusion subprocess is at work, with the γ^* always interacting with a c (or $\bar{c}$) sea quark, the average number of spectator valence quarks cannot depend significantly on Q^2. The same holds true for b (or $\bar{b}$) quarks.

Finally, the proton spectra of fig. 2a, obtained with LEPTO for all DIS events at different Q^2-values in the ep centre-of-mass frame, are again presented in fig. 5a but in the $\gamma^* p$ frame. At $x_F > 0$ the curves of fig. 5a compare well with the corresponding ones in fig. 2a. Namely the "leading effect" is still evident and the Q^2-dependence is similar. At $x_F < 0$, the spectra of fig. 5a show a small "shoulder" (around $x_F \sim -0.1$) which slightly grows as Q^2 increases. This shoulder contains the already mentioned "non-leading" protons from centrally produced $p\bar{p}$ pairs. In fact the corresponding antiproton spectra, shown in fig. 5b, are peaked exactly in the same x_F-region.

To summarize our results, in table 2 we give the average x_F-values vs. Q^2 relative to all secondary protons produced in the various conditions discussed so far.

---

2) We will further discuss this point in section 3 (see fig. 7).

3. TRANSVERSE MOMENTUM DISTRIBUTION OF SECONDARY PROTONS

Let us consider the transverse momentum distribution of protons produced in DIS final states, in terms of $1/\sigma_{ev} \cdot d\sigma/dp_T^2$. LEPTO, PYTHIA, and HERWIG predictions are shown in figs. 6a, 6b and 6c, respectively, for three x_F-intervals: $0 < x_F < 0.5$, $0.5 < x_F < 1$ and $0 < x_F < 1$ (i.e. the whole positive x_F-range). The results refer to the ep frame, with EHLQ1 structure functions. The predictions from the three event generators are quite different. LEPTO (fig. 6a) predicts higher p_T for protons with $x_F < 0.5$ than for protons with $x_F > 0.5$: the difference in slope of the corresponding distributions is significantly large. In PYTHIA (fig. 6b) this difference still exists, but smaller, while in HERWIG (fig. 6c) the p_T^2-distributions at low and high x_F are really the same. In fig. 6d the PYTHIA, LEPTO and HERWIG p_T^2-distributions relative to "leading" protons with $x_F > 0.5$ are superimposed for comparison: the HERWIG curve is much less steep than the other two which are degenerate. In the whole $x_F > 0$ range, the slope of the p_T^2-spectrum decreases when going from PYTHIA (fig. 6b) to LEPTO (fig. 6a) and to HERWIG (fig. 6c). Notice that the spectra corresponding to $0 < x_F < 1$ and $0 < x_F < 0.5$ are obviously almost the same since the bulk of secondary protons are produced at low x_F. The average p_T^2-values of the distributions presented in fig. 6 for $x_F > 0$ and $x_F > 0.5$, are reported in table 3.

The nature of the difference in p_T for protons having large and small x_F, as predicted by LEPTO and PYTHIA generators, seems to be clear enough. We know that at small x_B the γ^* mainly interacts with a sea quark (or antiquark) produced via gluon cascade. An example of QCD diagram is presented in fig. 7. Here we can see the gamma-gluon interaction in the top part of the diagram with the production of a sea $q_s\overline{q}_s$ pair. The upper gluon emits other gluons and looses its virtuality and transverse momentum. The lower gluon is absorbed by a valence quark q_v of the proton. The emitted gluons also are converted into $q_s\overline{q}_s$ pairs. On the last step, all produced quarks are converted into hadrons and the probability for two or three quarks to recombine into one hadron decreases exponentially with increasing rapidity gap between these quarks. So valence quarks most probably recombine with sea quarks from the lower part of the diagram in fig. 7, which have comparatively small transverse momenta. As a result, the average transverse momentum of "leading" secondary hadrons (protons with high x_F) should be comparatively small too. On the other hand, the production of secondary protons with small x_F is due to the fusion of sea quarks from the upper and middle parts of the diagram, so these protons should have higher transverse momenta.

Let us now study how the proton p_T varies as a function of Q^2, using first either LEPTO or HERWIG. Since the shapes of the p_T^2-spectra obtained with these two event generators turn out to be more or less Q^2-independent, we will focus the discussion on the average p_T^2. Figures 8a and 8b, corresponding to LEPTO and HERWIG, respectively, illustrate the variation of $<p_T^2>$ vs. Q^2 for protons with $0 < x_F < 0.5$, $0.5 < x_F < 1$ and $0 < x_F < 1$. Three Q^2-values are considered (7, 100 and 1000 GeV^2), as in section 2. Unless differently specified, the data refer to all DIS events and to the ep centre-of-mass frame. LEPTO and HERWIG results are quite similar: for protons produced at low x_F (and therefore for all protons), $<p_T^2>$ increases very rapidly with Q^2; for "leading" protons with higher x_F, $<p_T^2>$ does not practically depend on Q^2. Analogous results obtained with PYTHIA are shown in fig. 8c. They differ from LEPTO predictions, which can be partly related with the particular definition of Q^2 in PYTHIA.

The growth of $<p_T^2>$ for protons with $x_F < 0.5$ is mainly connected with pure kinematical reasons. When Q^2 increases, the transverse momentum of γ^* also increases. As a consequence, the $\gamma^* p$ frame (which is the physical one) acquires some transverse boost relative to the ep frame. This translates into an increase of transverse momentum in the ep frame for all secondaries produced at small x_F. For secondaries with large x_F, this effect is practically absent. To illustrate this point, in figs. 9a and 9b we present the predictions of LEPTO for $<p_T^2>$ vs. Q^2 in both ep and $\gamma^* p$ frames, for protons produced in the central and forward regions, separately. In the $\gamma^* p$ frame, the growth of $<p_T^2>$ with Q^2 for secondary protons with $x_F < 0.5$ (fig. 9a) is much weaker than in the ep frame and it is absent, as in the ep frame, for protons with $x_F > 0.5$ (fig. 9b). The results from LEPTO in the $\gamma^* p$ frame are summarized in fig. 10.

Let us turn now to heavy flavour production. Qualitatively the same $<p_T^2>$ vs. Q^2 trend applies to DIS events containing heavy flavours. Namely the values of $<p_T^2>$ do not depend on Q^2 for secondary protons with $x_F > 0.5$, as shown in figs. 11a and 11b for charm and beauty events generated with LEPTO. On the other hand, $<p_T^2>$ increases with Q^2 for protons at small x_F but not as strongly as in fig. 8a, relative to all DIS events.

In fact, assuming again that the main subprocess for heavy quark pair-production is $\gamma^* g \to Q\bar{Q}$, then the $Q\bar{Q}$ pair is produced in the upper part of the diagram shown in fig. 7. Since c or b-mesons are much more abundantly produced than c or b-baryons, fragmentation and recombination effects are such that the bulk of secondary protons (not coming from heavy baryon decays) are produced on the average closer to the "target" proton. Therefore physical as well as kinematical Q^2-effects for secondary protons in events with heavy flavours should be smaller.

Again, to summarize our results, the average p_T^2-values vs. Q^2 discussed in this section are reported all together in tables 3 and 4.

4. CONCLUSION

We have considered three Monte Carlo event generators based on QCD (PYTHIA, LEPTO and HERWIG) to simulate the production of secondary protons in ep Deep Inelastic Scattering at HERA energies.

All of them manifest the "leading proton effect", i.e. an abundant proton production at $x_F > 0$ in the ep centre-of-mass reference frame, with a sizable fraction of protons in the forward region at $x_F > 0.5$. When all DIS events (i.e. minimum bias events) are considered, this "leading effect" is more pronounced in LEPTO and PYTHIA than in HERWIG. In LEPTO and PYTHIA it decreases as Q^2 increases, more rapidly than in HERWIG. When only events containing heavy flavours (charm and beauty) are considered, the "leading effect" is also reduced, more in LEPTO than in either PYTHIA or HERWIG, almost independently from the heavy quark mass. In addition, as observed with LEPTO, there is no clear Q^2-dependence of the effect in this case.

As far as the proton transverse momentum is concerned, HERWIG predicts higher p_T than LEPTO and PYTHIA for all protons with positive x_F. For "leading" protons with $x_F > 0.5$, HERWIG predicts the same p_T as for all protons, while LEPTO and PYTHIA predict lower p_T (as one would expect, see section 3). In both LEPTO and HERWIG the p_T considerably increases with Q^2 for all protons, but for protons with $x_F > 0.5$ it turns out to be Q^2-independent in LEPTO and slightly decreasing with increasing Q^2 in HERWIG. The same features remain when heavy flavours are produced, although the above p_T-increase with Q^2 is much smaller. Finally, compared to the minimum bias case, in LEPTO the proton p_T increases with the mass of the produced heavy quark for all protons and in particular for "leading" protons at high x_F (see table 3). In PYTHIA and HERWIG there is no clear dependence on the mass.

All the differences observed herein among the results from the various QCD event generators are likely related to differences existing at the hadronization level. A detailed comparison with experimental data cannot but improve the existing Monte Carlo models.

ACKNOWLEDGEMENTS

We are grateful to Ya. I. Azimov, V. A. Khoze and M. G. Ryskin for interesting discussions.

Table 1

The average x_F-values of secondary protons produced in ep interactions at $\sqrt{s} = 314$ GeV calculated with LEPTO, PYTHIA and HERWIG using EHLQ1 [33] or MT(S-DIS) [34] structure functions, for all DIS events (i.e. minimum bias) and for events with charm and beauty. The data refer to the ep centre-of-mass frame.

	$< x_F >$ LEPTO	$< x_F >$ PYTHIA	$< x_F >$ HERWIG
EHLQ1, all	0.276 ± 0.003	0.267 ± 0.004	0.203 ± 0.002
MT(S-DIS), all	0.259 ± 0.003	0.265 ± 0.003	0.202 ± 0.006
EHLQ1, with $c\bar{c}$	0.179 ± 0.002	0.237 ± 0.002	0.190 ± 0.002
EHLQ1, with $b\bar{b}$	0.172 ± 0.008	0.235 ± 0.002	0.182 ± 0.002

Table 2

The average x_F-values of secondary protons produced in ep interactions at $\sqrt{s} = 314$ GeV calculated with LEPTO and HERWIG using EHLQ1 [33] structure functions, for different values of Q^2. The data refer to all DIS events (i.e minimum bias) and to events with charm and beauty production. Both the ep and $\gamma^* p$ centre-of-mass frames are considered, as specified.

Q^2 [GeV^2]	$< x_F >$ LEPTO	$< x_F >$ HERWIG
All, ep frame		
7	0.279 ± 0.002	0.204 ± 0.002
100	0.247 ± 0.002	0.196 ± 0.002
1000	0.223 ± 0.002	0.183 ± 0.002
With $c\bar{c}$, ep frame		
7	0.179 ± 0.001	-
100	0.183 ± 0.001	-
1000	0.185 ± 0.001	-
With $b\bar{b}$, ep frame		
7	0.16 ± 0.01	-
100	0.184 ± 0.007	-
1000	0.177 ± 0.005	-
All, $\gamma^* p$ frame		
7	0.316 ± 0.002	-
100	0.276 ± 0.002	-
1000	0.245 ± 0.002	-

Table 3

The average p_T^2-values of secondary protons produced in ep interactions at $\sqrt{s} = 314$ GeV calculated with LEPTO, PYTHIA and HERWIG using EHLQ1 [33] structure functions, for all DIS events (i.e. minimum bias) and for events with charm and beauty. The data refer to the ep centre-of-mass frame.

	LEPTO $< p_T^2 >$ [GeV^2]	PYTHIA $< p_T^2 >$ [GeV^2]	HERWIG $< p_T^2 >$ [GeV^2]
All			
$0 < x_F < 1$	0.65 ± 0.03	0.38 ± 0.02	0.75 ± 0.01
$0.5 < x_F < 1$	0.27 ± 0.01	0.27 ± 0.01	0.76 ± 0.02
With $c\bar{c}$			
$0 < x_F < 1$	0.57 ± 0.02	0.33 ± 0.01	0.63 ± 0.01
$0.5 < x_F < 1$	0.37 ± 0.02	0.24 ± 0.01	0.63 ± 0.05
With $b\bar{b}$			
$0 < x_F < 1$	0.85 ± 0.12	0.58 ± 0.03	0.72 ± 0.02
$0.5 < x_F < 1$	1.0 ± 0.3	0.26 ± 0.04	0.54 ± 0.04

Table 4

The average p_T^2-values of secondary protons produced in ep interactions at $\sqrt{s} = 314$ GeV calculated with LEPTO and HERWIG using EHQL1 [33] structure functions, for different values of Q^2. The data refer to all DIS events (i.e minimum bias) and to events with charm and beauty, in the ep centre-of-mass frame.

	Q^2 [GeV^2]	x_F	LEPTO $< p_T^2 >$ [GeV^2]	HERWIG $< p_T^2 >$ [GeV^2]
All	7	$0 \div 1$	0.43 ± 0.01	0.63 ± 0.01
	7	$0.5 \div 1$	0.28 ± 0.04	0.85 ± 0.02
	100	$0 \div 1$	1.33 ± 0.04	1.33 ± 0.02
	100	$0.5 \div 1$	0.30 ± 0.03	0.69 ± 0.02
	1000	$0 \div 1$	3.7 ± 0.1	3.47 ± 0.01
	1000	$0.5 \div 1$	0.27 ± 0.01	0.64 ± 0.02
With $c\bar{c}$	7	$0 \div 1$	0.42 ± 0.01	-
	7	$0.5 \div 1$	0.32 ± 0.01	-
	100	$0 \div 1$	0.80 ± 0.02	-
	100	$0.5 \div 1$	0.31 ± 0.01	-
	1000	$0 \div 1$	2.04 ± 0.07	-
	1000	$0.5 \div 1$	0.35 ± 0.02	-
With $b\bar{b}$	7	$0 \div 1$	0.63 ± 0.01	-
	7	$0.5 \div 1$	0.38 ± 0.04	-
	100	$0 \div 1$	0.82 ± 0.06	-
	100	$0.5 \div 1$	0.39 ± 0.08	-
	1000	$0 \div 1$	1.86 ± 0.1	-
	1000	$0.5 \div 1$	0.29 ± 0.02	-

Figure captions

Fig. 1 : x_F-distributions for secondary protons produced in ep interactions at $\sqrt{s} = 314$ GeV, as obtained with LEPTO, PYTHIA and HERWIG: all protons with EHLQ1 structure functions (a); all protons with MT (S-DIS) structure functions (b); "leading" protons with EHLQ1 structure functions (c); same as (a) without x_E-scaling (d).

Fig. 2 : x_F-distributions in the ep centre-of-mass frame for all secondary protons produced in ep interactions at $\sqrt{s} = 314$ GeV and different Q^2-values, as obtained with LEPTO (a), HERWIG (b) and PYTHIA (c) using EHLQ1 structure functions.

Fig. 3 : x_F-distributions in the ep centre-of-mass frame for all secondary protons produced in ep interactions at $\sqrt{s} = 314$ GeV in events with charm (a) and beauty (b), as obtained with LEPTO, PYTHIA and HERWIG using EHLQ1 structure functions.

Fig. 4 : x_F-distributions in the ep centre-of-mass frame for all secondary protons produced in ep interactions at $\sqrt{s} = 314$ GeV and different Q^2-values in events with charm, as obtained with LEPTO using EHLQ1 structure functions.

Fig. 5 : x_F-distributions in the $\gamma^* p$ centre-of-mass frame for all secondary protons (a) and antiprotons (b) produced in ep interactions at $\sqrt{s} = 314$ GeV and different Q^2-values, as obtained with LEPTO using EHLQ1 structure functions.

Fig. 6 : p_T^2-distributions in the ep centre-of-mass frame for all secondary protons produced in ep interactions at $\sqrt{s} = 314$ GeV in different x_F-regions, as obtained with LEPTO (a), PYTHIA (b) and HERWIG (c) using EHLQ1 structure functions; in the forward region ($0.5 < x_F < 1$), the LEPTO, PYTHIA and HERWIG distributions are also shown together for comparison (d).

Fig. 7 : An example of QCD diagram for ep DIS at small x_B.

Fig. 8 : $< p_T^2 >$ vs. Q^2 in the ep centre-of-mass frame for all secondary protons produced in ep interactions at $\sqrt{s} = 314$ GeV in different x_F-regions, as obtained with LEPTO (a), HERWIG (b) and PYTHIA (c) using EHLQ1 structure functions.

Fig. 9 : $<p_T^2>$ vs. Q^2 in the ep and $\gamma^* p$ centre-of-mass frames for all secondary protons produced in ep interactions at $\sqrt{s} = 314$ GeV with $0 < x_F < 0.5$ (a) and $0.5 < x_F < 1$ (b), as obtained with LEPTO using EHLQ1 structure functions.

Fig. 10 : $<p_T^2>$ vs. Q^2 in the $\gamma^* p$ centre-of-mass frame for all secondary protons produced in ep interactions at $\sqrt{s} = 314$ GeV in different x_F-regions, as obtained with LEPTO using EHLQ1 structure functions.

Fig. 11 : $<p_T^2>$ vs. Q^2 in the ep centre-of-mass frame for all secondary protons produced in ep interactions at $\sqrt{s} = 314$ GeV in different x_F-regions when charm (a) and

beauty (b) are also produced, as obtained with LEPTO using EHLQ1 structure functions.

REFERENCES

[1] ZEUS Collaboration (M. Derrick et al.): "The ZEUS Detector: Status Report 1989", DESY PRC 89-01 (March 1989).

[2] M. Basile, G Cara Romeo, L. Cifarelli, A. Contin, G. D'Ali, P. Di Cesare, B. Esposito, P. Giusti, T. Massam, F. Palmonari, G. Sartorelli, G. Valenti and A. Zichichi, Phys. Lett. 92B (1980) 367.

[3] M. Basile et al., Nuovo Cimento 58A (1980) 193.

[4] M. Basile et al., Phys. Lett. 95B (1980) 311.

[5] M. Basile et al., Lettere al Nuovo Cimento 29 (1980) 491.

[6] M. Basile et al., Phys. Lett. 99B (1981) 247.

[7] M. Basile et al., Lettere al Nuovo Cimento 30 (1981) 389.

[8] M. Basile et al., Lettere al Nuovo Cimento 31 (1981) 273.

[9] M. Basile et al., Nuovo Cimento 65A (1981) 400.

[10] M. Basile et al., Nuovo Cimento 65A (1981) 414.

[11] M. Basile et al., Lettere al Nuovo Cimento 32 (1981) 210.

[12] M. Basile et al., Lettere al Nuovo Cimento 32 (1981) 321.

[13] M. Basile et al., Nuovo Cimento 66A (1981) 129.

[14] M. Basile et al., Nuovo Cimento 67A (1982) 53.

[15] M. Basile et al., Nuovo Cimento 67A (1982) 244.

[16] M. Basile et al., Nuovo Cimento 73A (1983) 329.

[17] M. Basile et al., Lettere al Nuovo Cimento 36 (1983) 303.

[18] M. Basile et al., Lettere al Nuovo Cimento 36 (1983) 555.

[19] M. Basile et al., Lettere al Nuovo Cimento 36 (1983) 563.

[20] M. Basile et al., Lettere al Nuovo Cimento 37 (1983) 246.

[21] M. Basile et al., Lettere al Nuovo Cimento 37 (1983) 289.

[22] M. Basile et al., Lettere al Nuovo Cimento 38 (1983) 289.

[23] M. Basile et al., Lettere al Nuovo Cimento 38 (1983) 359.

[24] M. Basile et al., Lettere al Nuovo Cimento 38 (1983) 367.

[25] M. Basile et al., Nuovo Cimento 79A (1984) 1.

[26] M. Basile et al., Lettere al Nuovo Cimento 41 (1984) 293.

[27] M. Basile et al., Lettere al Nuovo Cimento 41 (1984) 298.

[28] G. Ingelman, Proc. of the Workshop on "Physics at HERA", DESY, Hamburg, Germany, 29-30 October 1991 (Ed. W. Buchmüller and G. Ingelman), v.3, p. 1366, and preprint TSL ISV 92-0065 (1992).

[29] G. Marchesini and B. R. Webber, Nucl. Phys B130 (1988) 571.

[30] T. Sjöstrand, Comp. Phys. Comm. 39 (1986) 347; T. Sjöstrand and M. Bengtsson, Comp. Phys. Comm. 43 (1987) 367; H. U. Bengtsson and T. Sjöstrand, Comp. Phys. Comm. 46 (1987) 43; T. Sjöstrand and M. van Zijl, Phys. Rev. D36 (1987) 2019; T. Sjöstrand, preprint CERN-TH.6488/92, May 1992.

[31] F. Anselmo, L. Cifarelli, E. Eskut and Yu. M. Shabelski, Nuovo Cimento 105A (1992) 1371.

[32] EMC Collaboration (M.Arneodo et al.), Z. Phys. C35 (1987) 433.

[33] E. Eichten, I. Hinchliffe, K. Lane and C. Quigg, Rev. Mod. Phys. 56 (1984) 579; 58 (1985) 1065.

[34] J. G. Morfin and W.-K. Tung, Z. Phys. C52 (1991) 13.

[35] L. Cifarelli, E. Eskut and Yu. M. Shabelski, Nuovo Cimento 106A (1993) 389.
[36] L. Cifarelli, Yu. M. Shabelski and O. P. Strogova: "Monte Carlo simulations for leading proton production in pp interactions up to $\sqrt{s} = 200$ TeV", preprint EMCSC, in preparation.

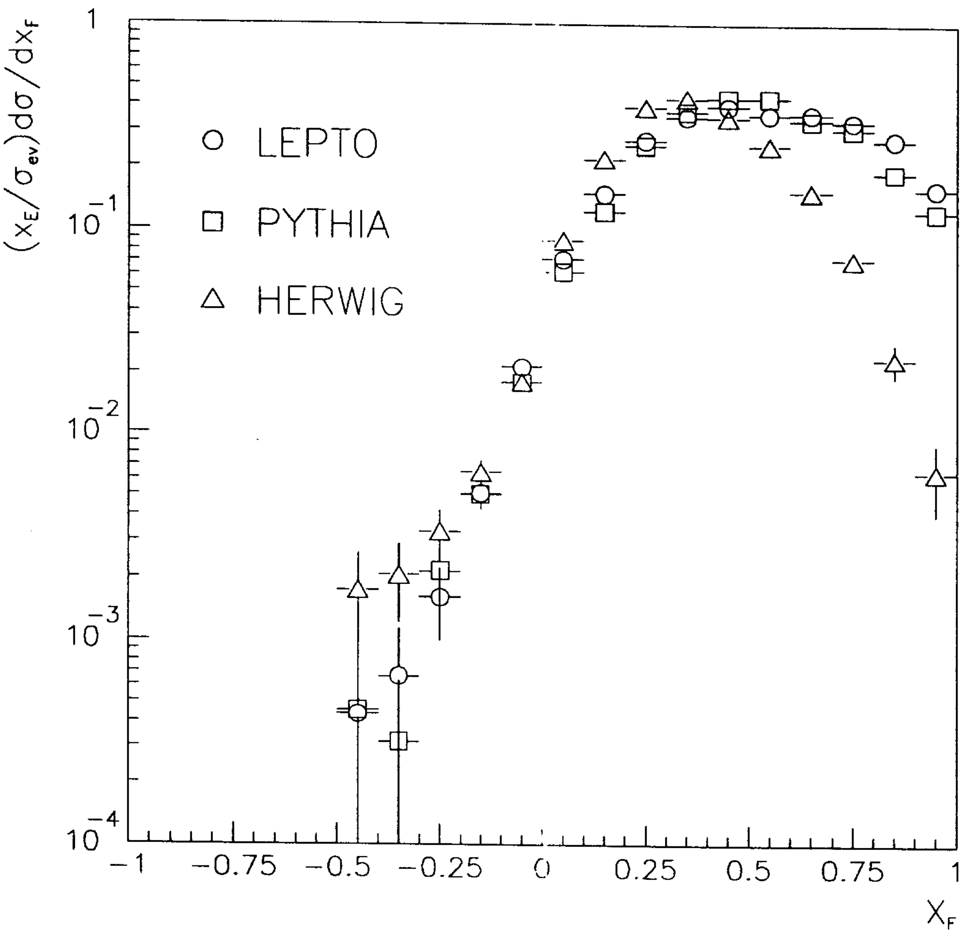

$(x_E/\sigma_{ev})d\sigma/dx_F$
1
10^{-1}
10^{-2}
10^{-3}
10^{-4}
LEPTO
PYTHIA
HERWIG
−1
−0.75
−0.5
−0.25
0
0.25
0.5
0.75
1
X_F

Fig.1a

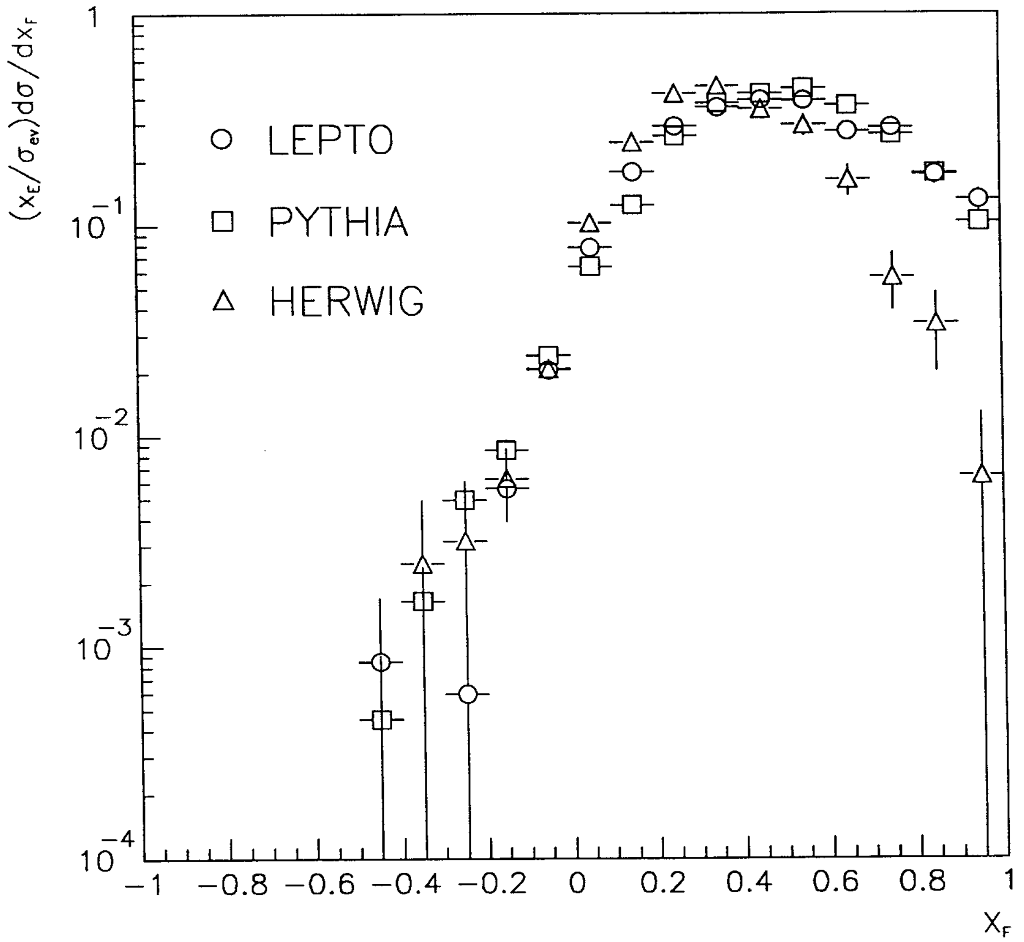

(x_E/σ_ev)dσ/dx_F
1
10^-1
10^-2
10^-3
10^-4
LEPTO
PYTHIA
HERWIG
−1 −0.8 −0.6 −0.4 −0.2 0 0.2 0.4 0.6 0.8 1
X_F

Fig.1b

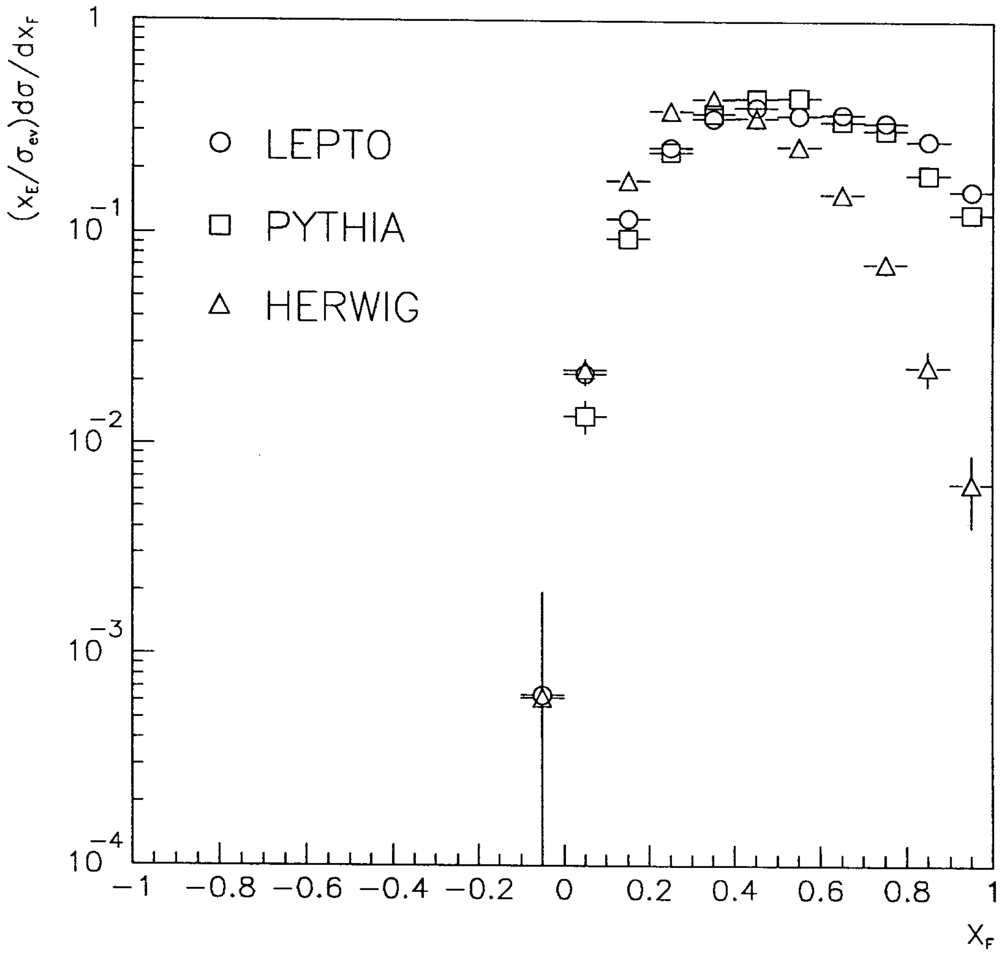

$(x_E/\sigma_{ev})d\sigma/dx_F$
1
10^{-1}
10^{-2}
10^{-3}
10^{-4}
LEPTO
PYTHIA
HERWIG
−1 −0.8 −0.6 −0.4 −0.2 0 0.2 0.4 0.6 0.8 1
x_F

Fig.1c

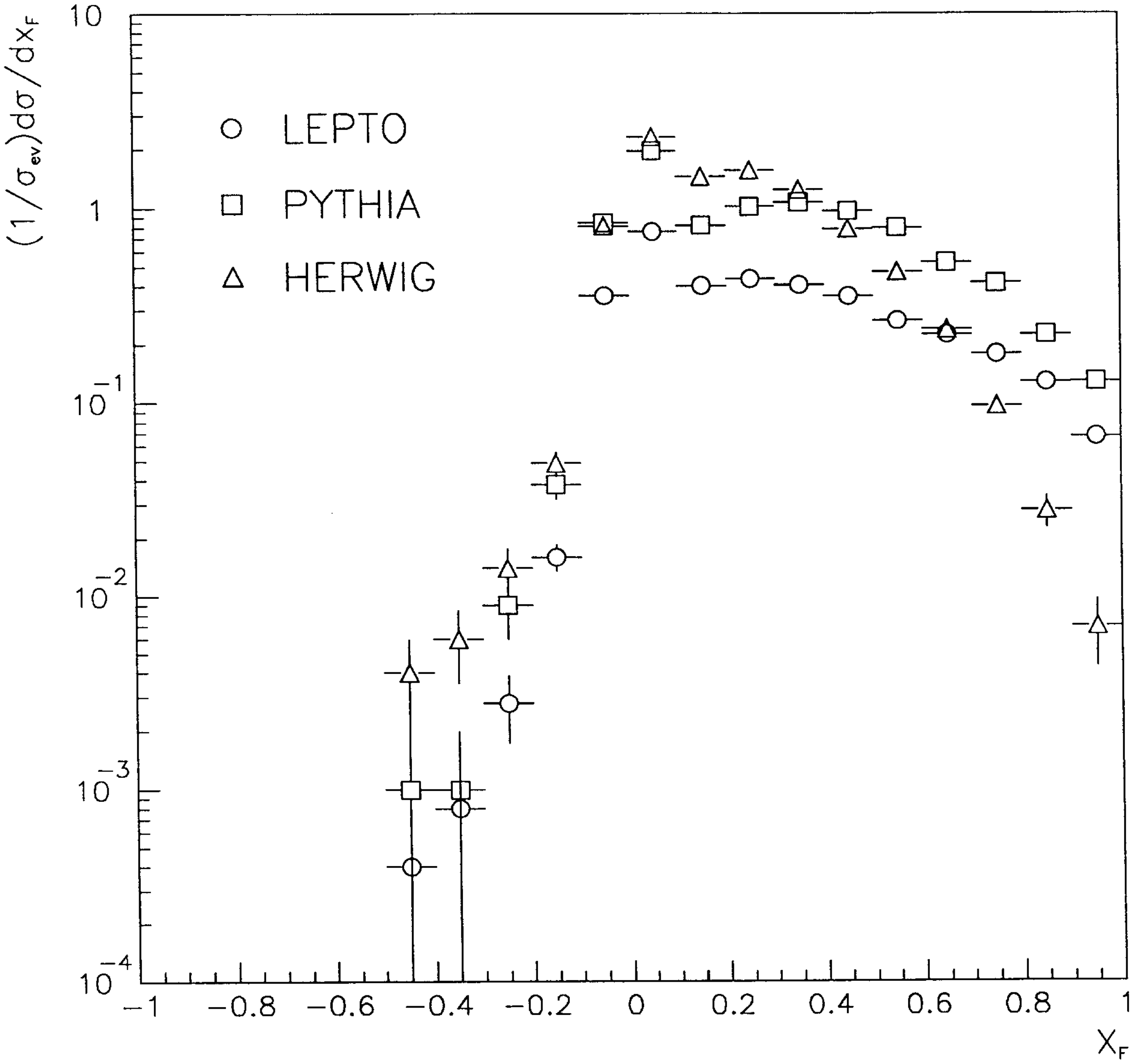

$(1/\sigma_{ev})d\sigma/dx_F$
10
1
10^{-1}
10^{-2}
10^{-3}
10^{-4}
LEPTO
PYTHIA
HERWIG
−1
−0.8
−0.6
−0.4
−0.2
0
0.2
0.4
0.6
0.8
1
X_F

Fig.1d

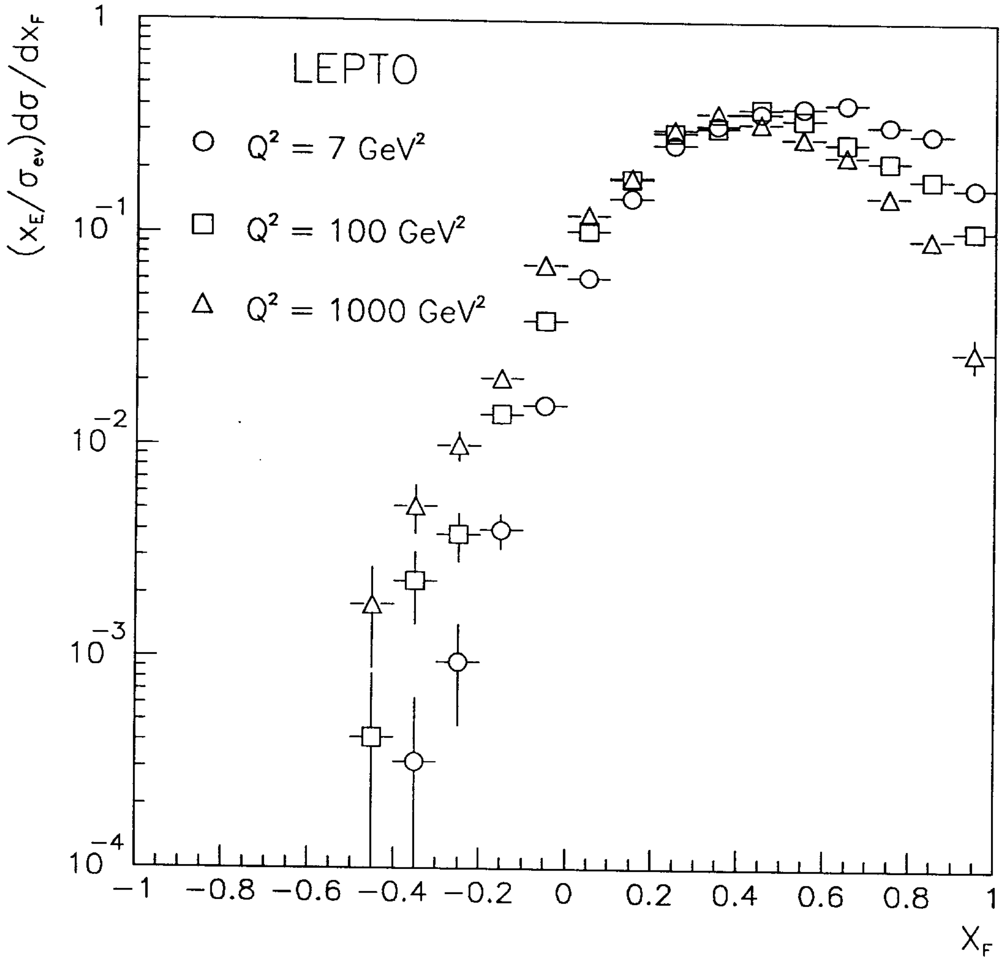
LEPTO
Q^2 = 7 GeV^2
Q^2 = 100 GeV^2
Q^2 = 1000 GeV^2
$(x_E/\sigma_{ev})d\sigma/dx_F$
X_F
1
10^{-1}
10^{-2}
10^{-3}
10^{-4}
−1 −0.8 −0.6 −0.4 −0.2 0 0.2 0.4 0.6 0.8 1

Fig.2a

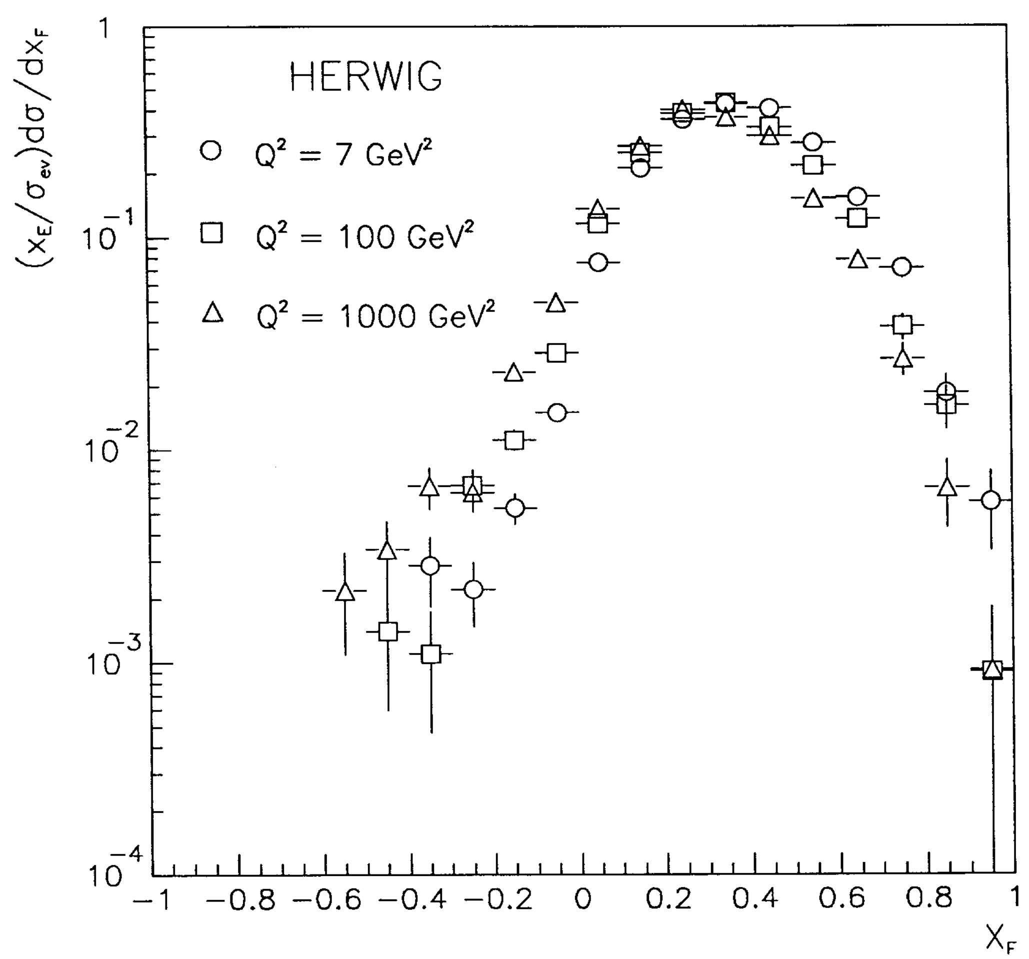

HERWIG
$Q^2 = 7$ GeV^2
$Q^2 = 100$ GeV^2
$Q^2 = 1000$ GeV^2
$(x_E/\sigma_{ev})d\sigma/dx_F$
x_F
1
10^{-1}
10^{-2}
10^{-3}
10^{-4}
−1 −0.8 −0.6 −0.4 −0.2 0 0.2 0.4 0.6 0.8 1

Fig.2b

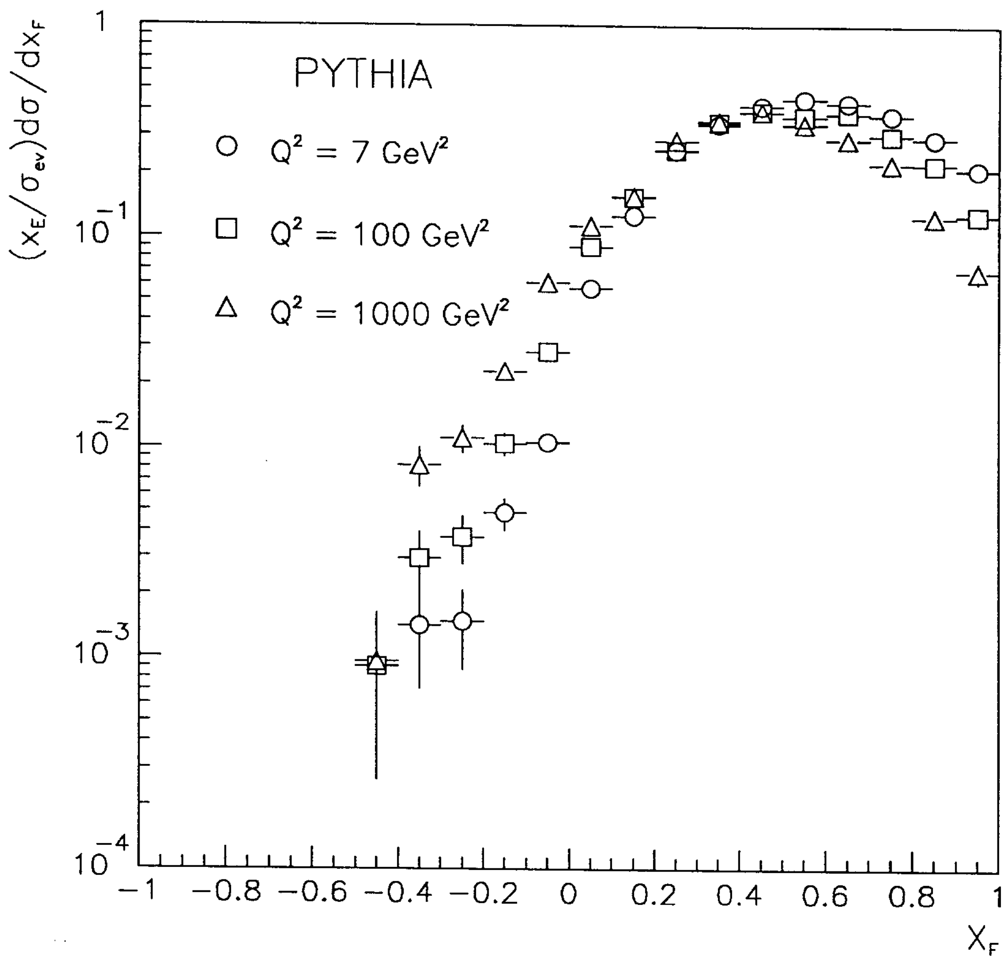

PYTHIA
Q² = 7 GeV²
Q² = 100 GeV²
Q² = 1000 GeV²
(x_E/σ_ev)dσ/dx_F
X_F
1
10⁻¹
10⁻²
10⁻³
10⁻⁴
−1
−0.8
−0.6
−0.4
−0.2
0
0.2
0.4
0.6
0.8
1

Fig.2c

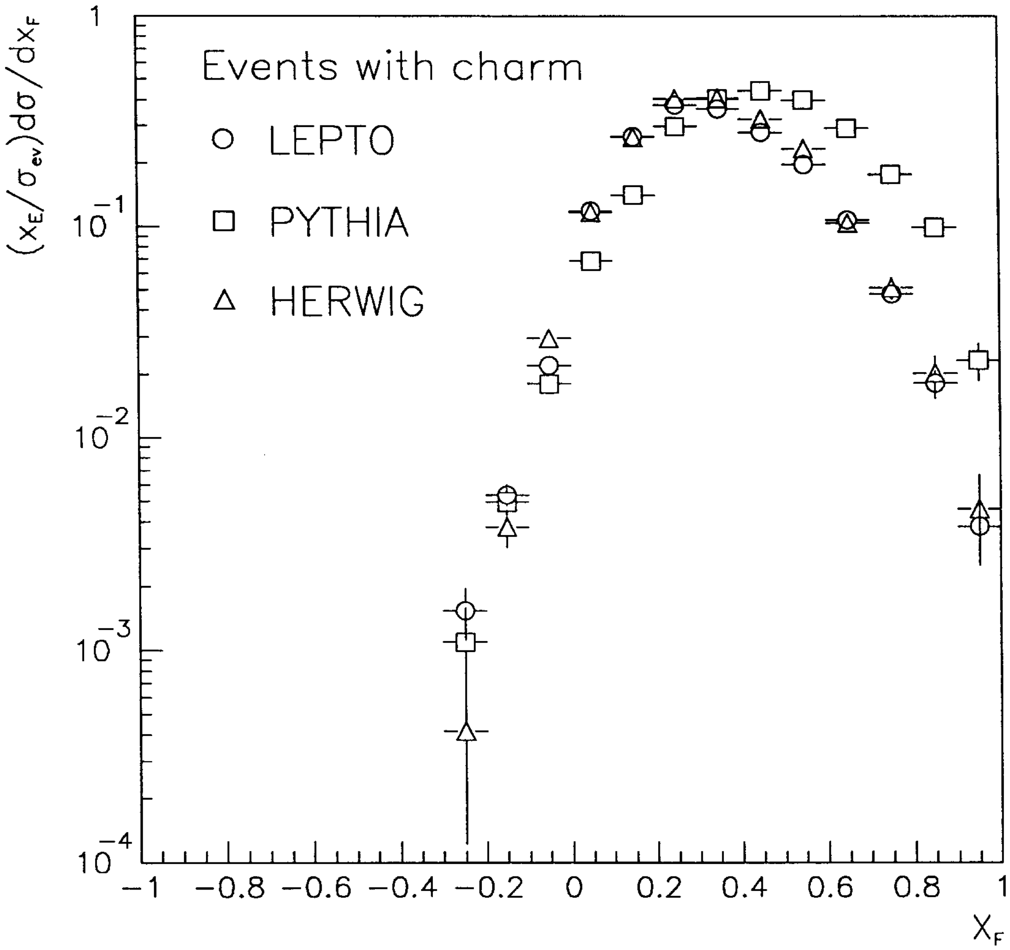
Events with charm
LEPTO
PYTHIA
HERWIG
$(x_E/\sigma_{ev})d\sigma/dx_F$
x_F
1
10^{-1}
10^{-2}
10^{-3}
10^{-4}
−1 −0.8 −0.6 −0.4 −0.2 0 0.2 0.4 0.6 0.8 1

Fig.3a

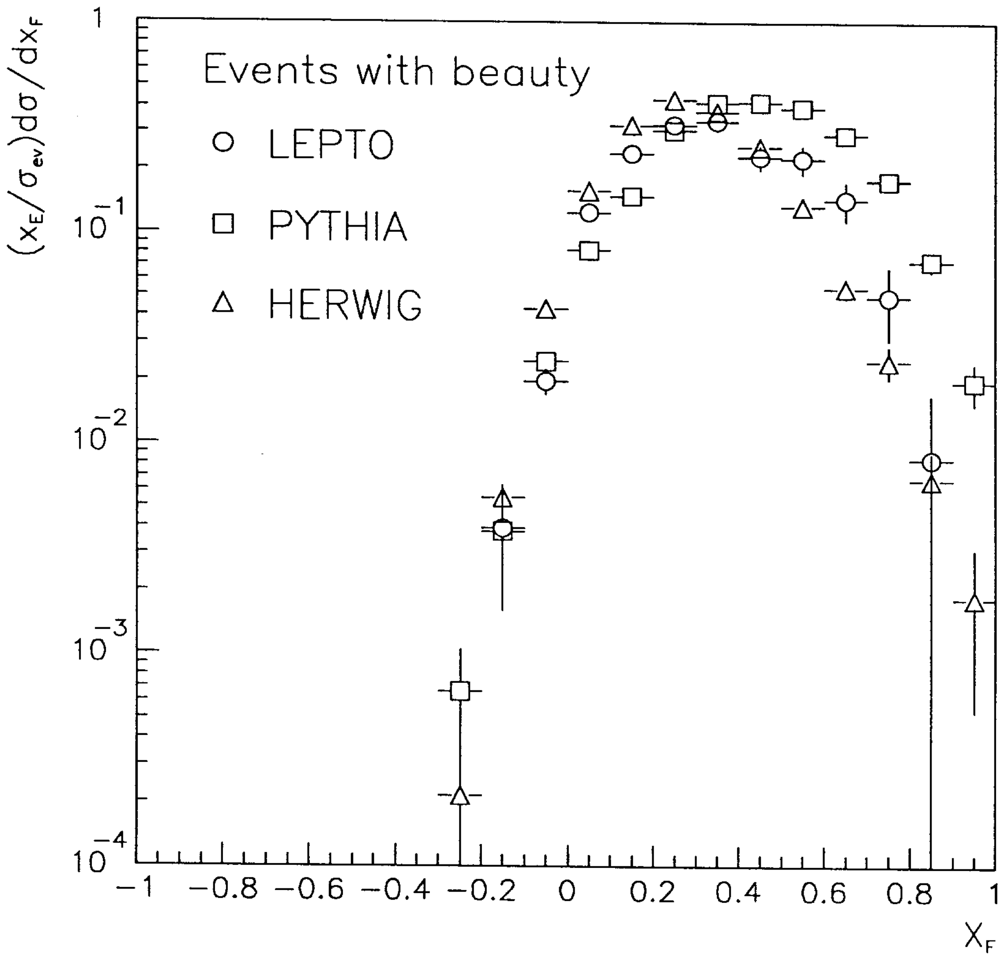

Events with beauty
LEPTO
PYTHIA
HERWIG
$(x_E/\sigma_{ev})d\sigma/dx_F$
1
10^{-1}
10^{-2}
10^{-3}
10^{-4}
−1 −0.8 −0.6 −0.4 −0.2 0 0.2 0.4 0.6 0.8 1
X_F

Fig.3b

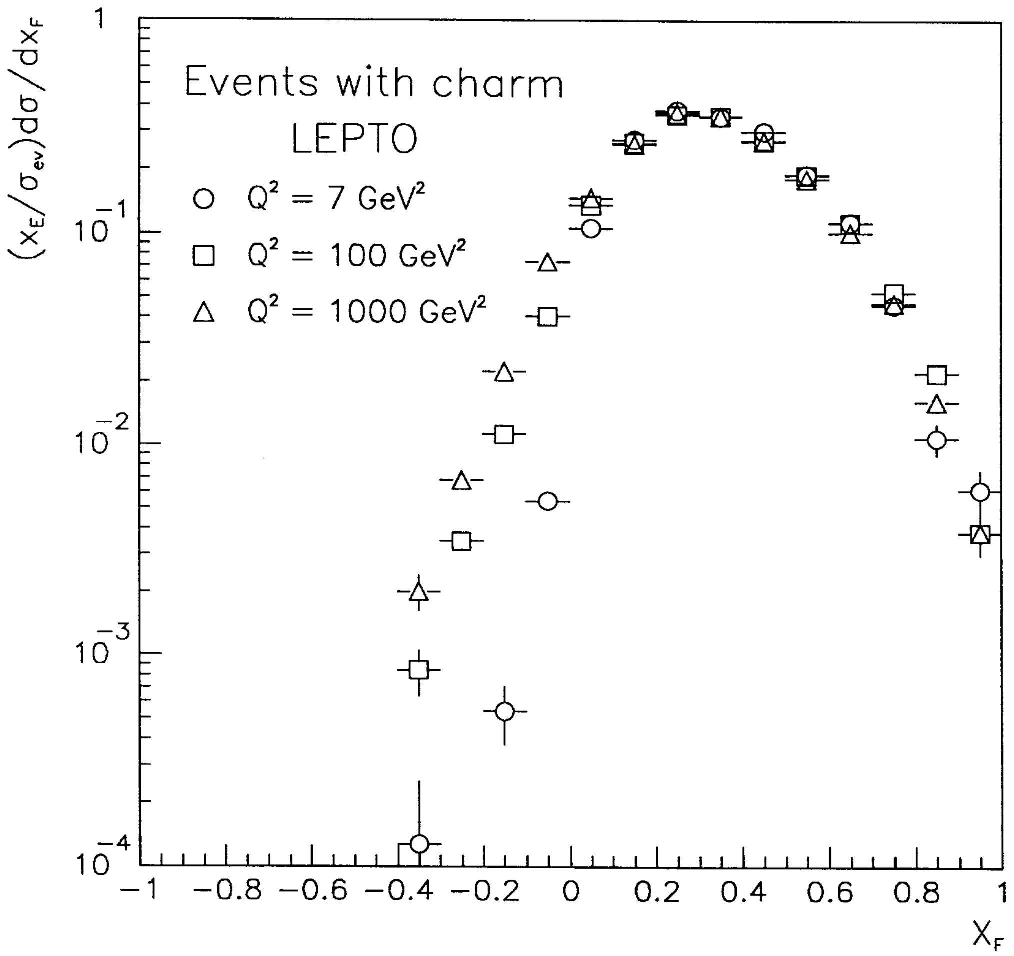

Events with charm
LEPTO
Q^2 = 7 GeV^2
Q^2 = 100 GeV^2
Q^2 = 1000 GeV^2
$(x_E/\sigma_{ev})d\sigma/dx_F$
X_F
1
10^{-1}
10^{-2}
10^{-3}
10^{-4}
−1
−0.8
−0.6
−0.4
−0.2
0
0.2
0.4
0.6
0.8
1

Fig.4

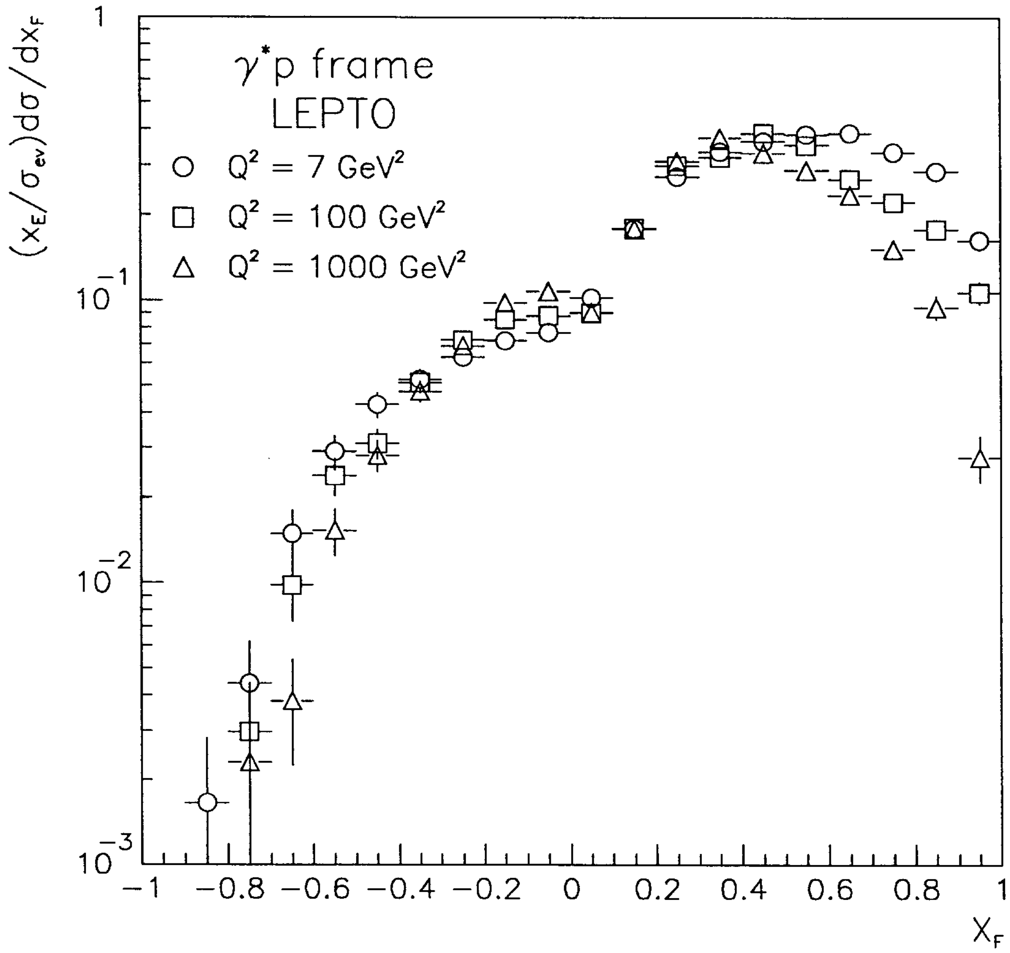

γ^*p frame
LEPTO
Q^2 = 7 GeV^2
Q^2 = 100 GeV^2
Q^2 = 1000 GeV^2
$(x_E/\sigma_{ev})d\sigma/dx_F$
1
10^{-1}
10^{-2}
10^{-3}
−1
−0.8
−0.6
−0.4
−0.2
0
0.2
0.4
0.6
0.8
1
X_F

Fig.5a

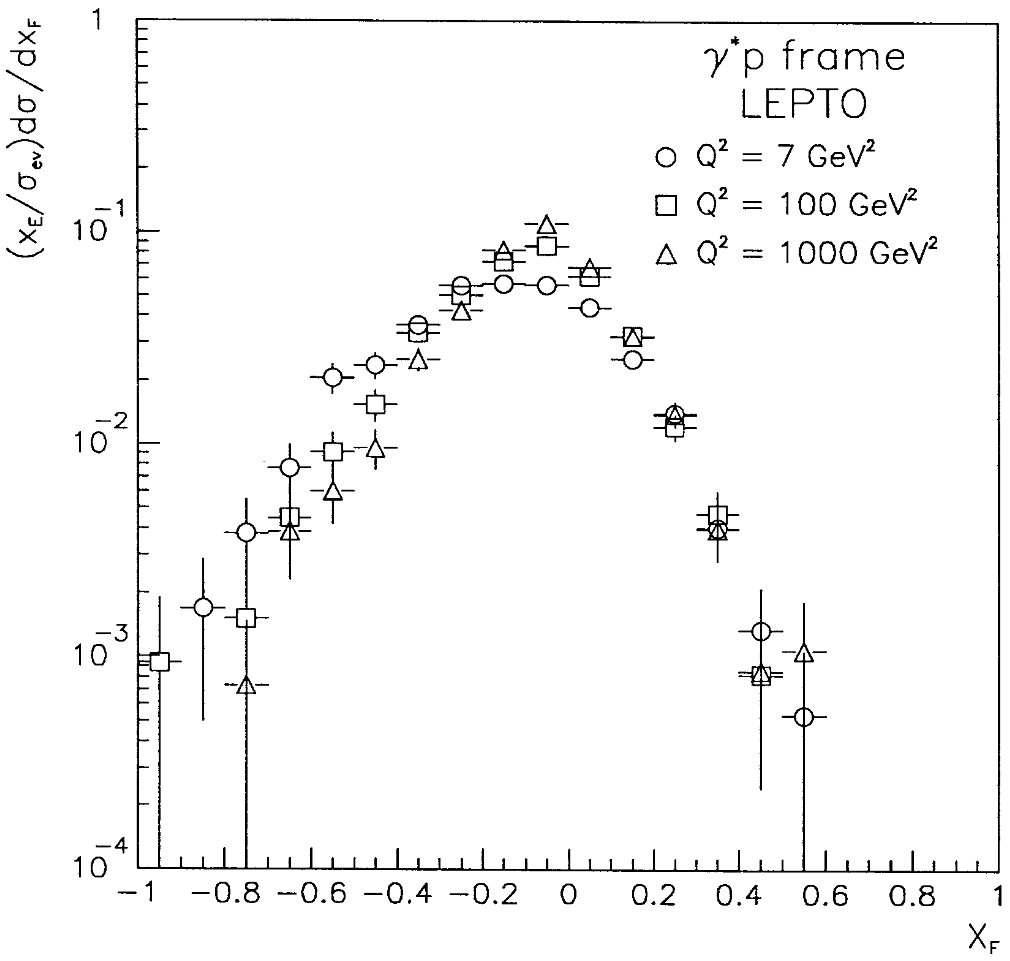

γ^*p frame
LEPTO
○ Q^2 = 7 GeV^2
□ Q^2 = 100 GeV^2
△ Q^2 = 1000 GeV^2
$(x_E/\sigma_{ev})d\sigma/dx_F$
1
10^{-1}
10^{-2}
10^{-3}
10^{-4}
−1 −0.8 −0.6 −0.4 −0.2 0 0.2 0.4 0.6 0.8 1
X_F

Fig.5b

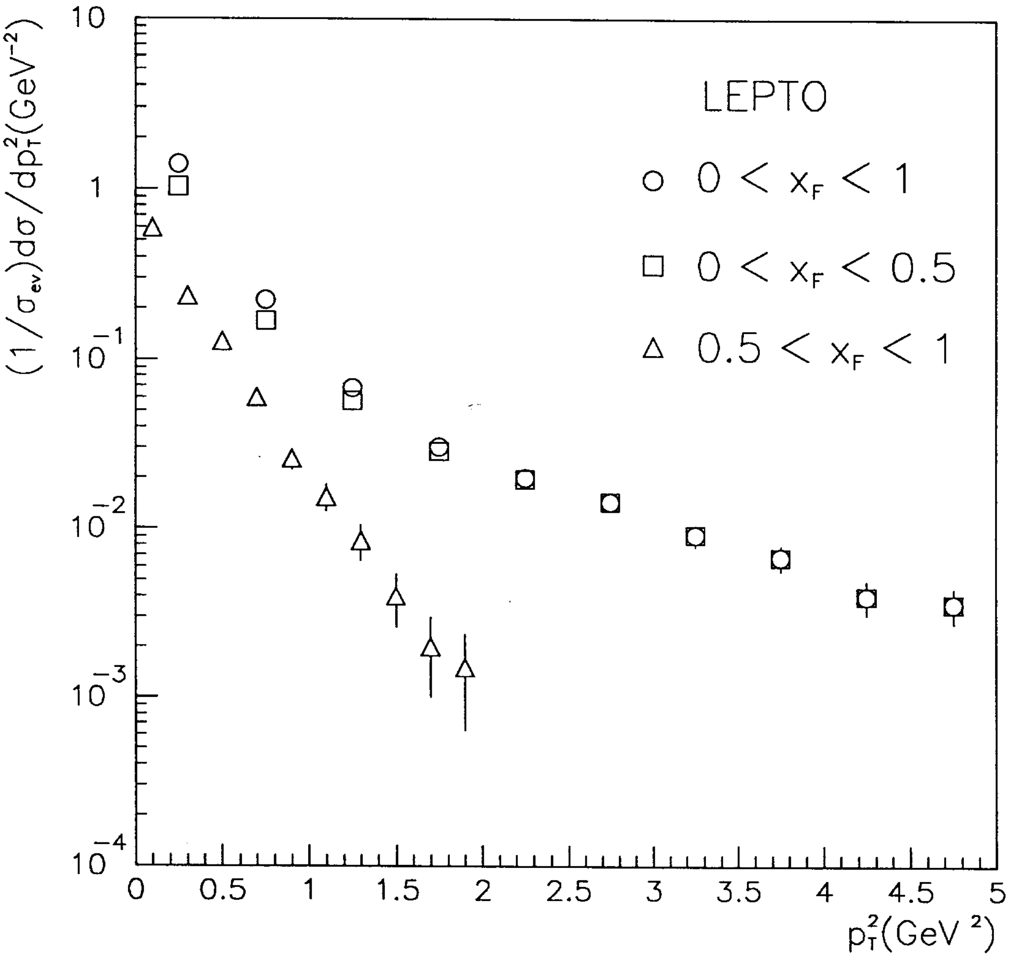

$(1/\sigma_{ev})d\sigma/dp_T^2(GeV^{-2})$
10
1
10^{-1}
10^{-2}
10^{-3}
10^{-4}
LEPTO
$0 < x_F < 1$
$0 < x_F < 0.5$
$0.5 < x_F < 1$
0
0.5
1
1.5
2
2.5
3
3.5
4
4.5
5
$p_T^2(GeV^2)$

Fig. 6a

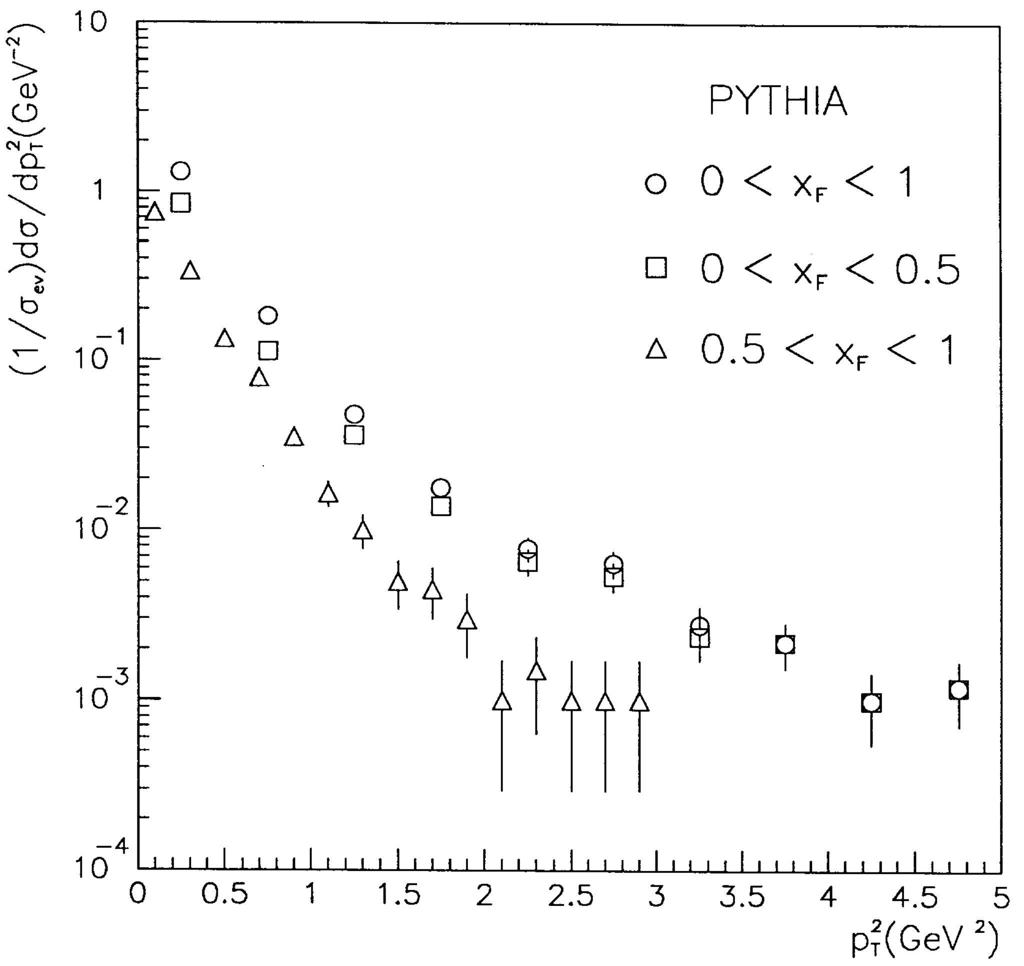

PYTHIA
0 < x_F < 1
0 < x_F < 0.5
0.5 < x_F < 1
(1/σ_ev)dσ/dp_T^2(GeV^-2)
p_T^2(GeV^2)
10
1
10^-1
10^-2
10^-3
10^-4
0
0.5
1
1.5
2
2.5
3
3.5
4
4.5
5

Fig. 6b

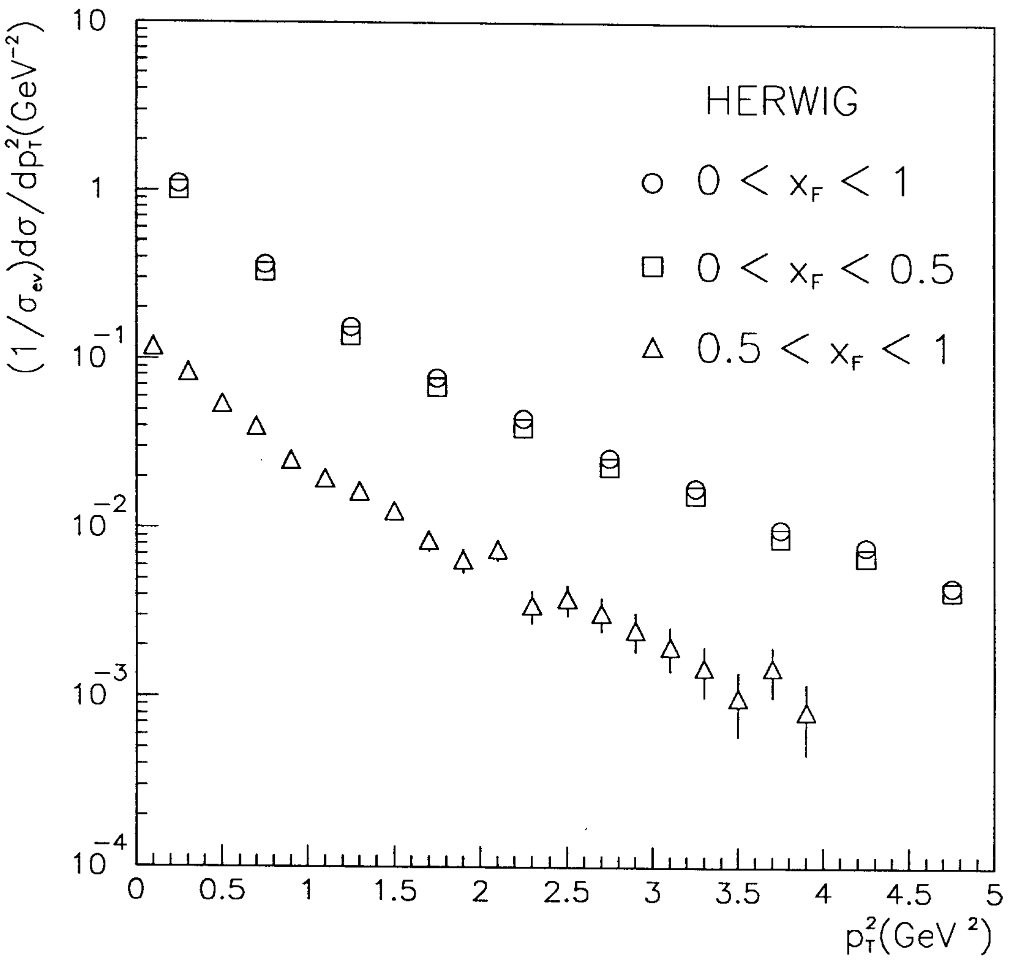
HERWIG
$0 < x_F < 1$
$0 < x_F < 0.5$
$0.5 < x_F < 1$
$(1/\sigma_{ev})d\sigma/dp_T^2(GeV^{-2})$
10
1
10^{-1}
10^{-2}
10^{-3}
10^{-4}
0 0.5 1 1.5 2 2.5 3 3.5 4 4.5 5
$p_T^2(GeV^2)$

Fig.6c

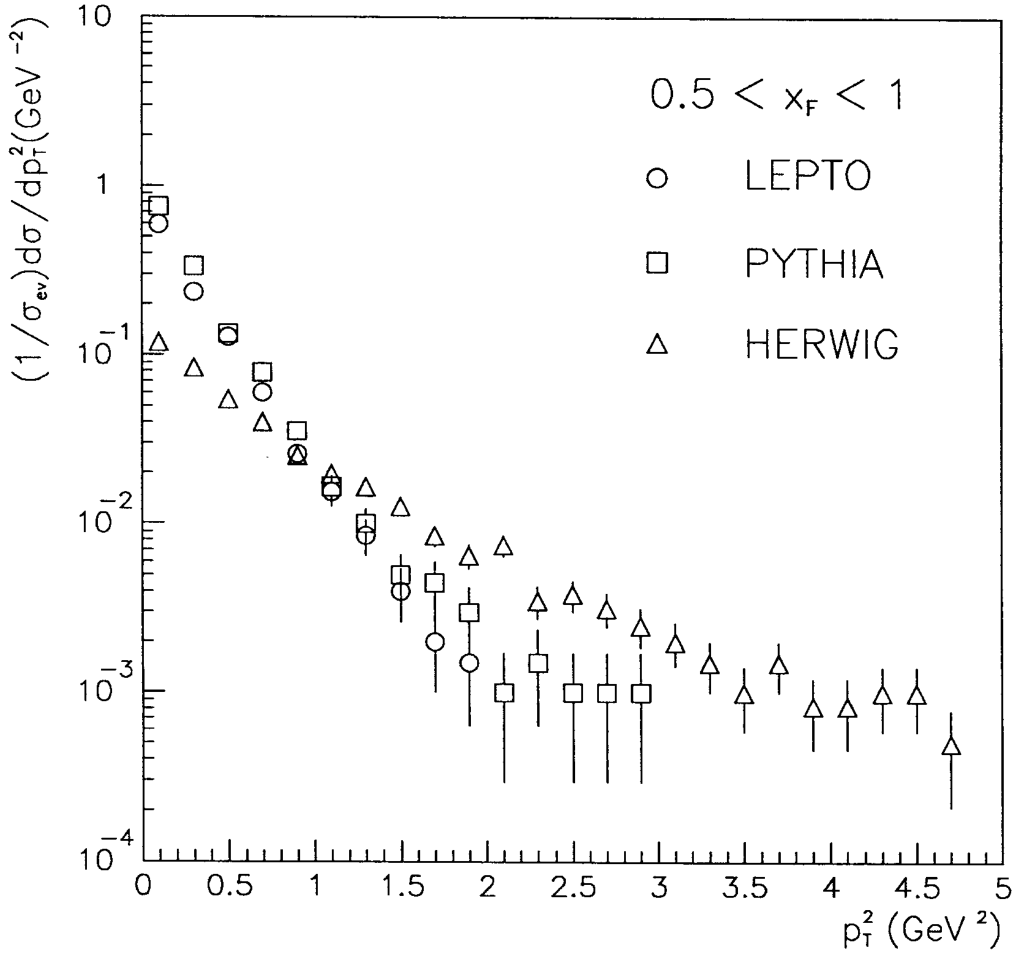
$0.5 < x_F < 1$
LEPTO
PYTHIA
HERWIG
$(1/\sigma_{ev})d\sigma/dp_T^2(GeV^{-2})$
p_T^2 (GeV ^{2})
10
1
10^{-1}
10^{-2}
10^{-3}
10^{-4}
0
0.5
1
1.5
2
2.5
3
3.5
4
4.5
5

Fig. 6d

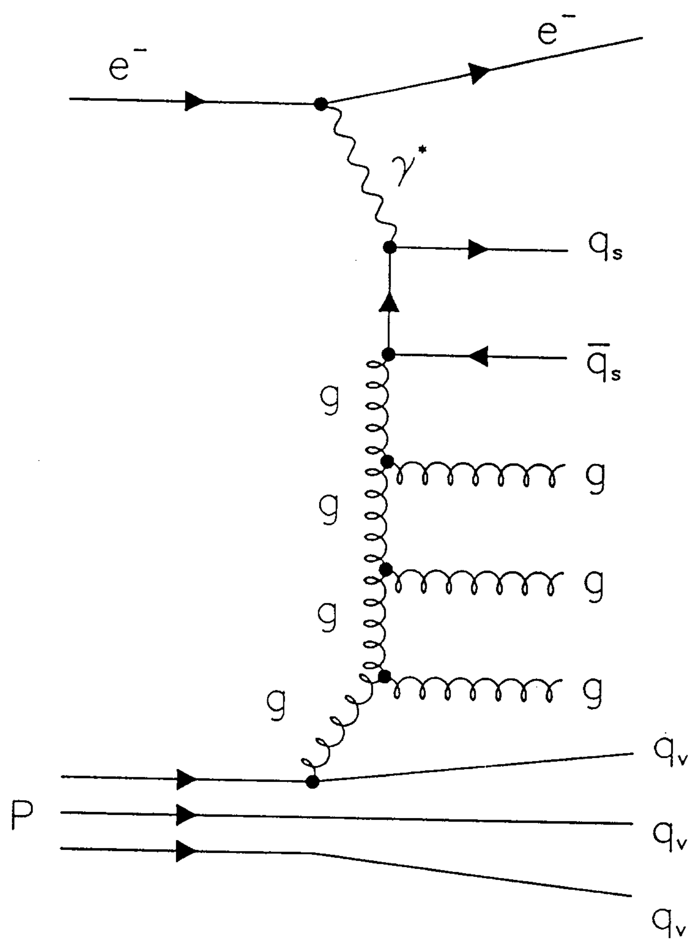

Fig.7

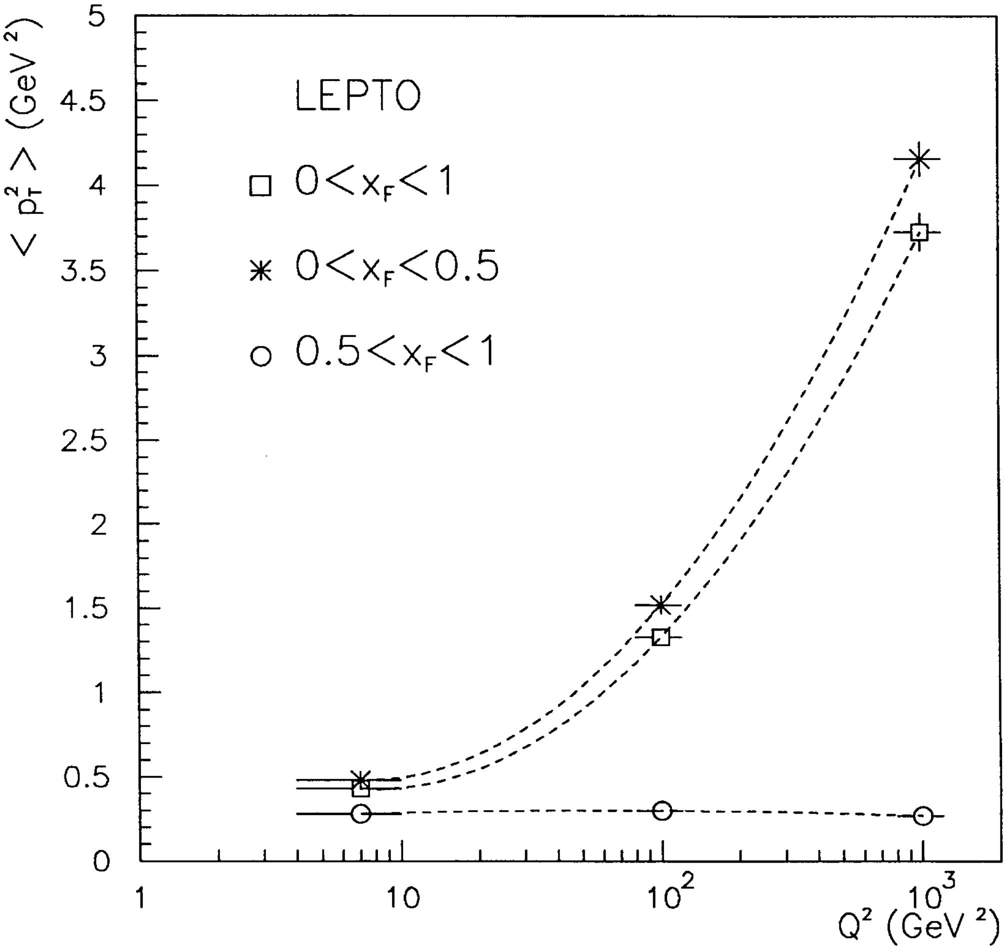

LEPTO
0<x_F<1
0<x_F<0.5
0.5<x_F<1
< p_T^2 > (GeV^2)
Q^2 (GeV^2)
0
0.5
1
1.5
2
2.5
3
3.5
4
4.5
5
1
10
10^2
10^3

Fig. 8a

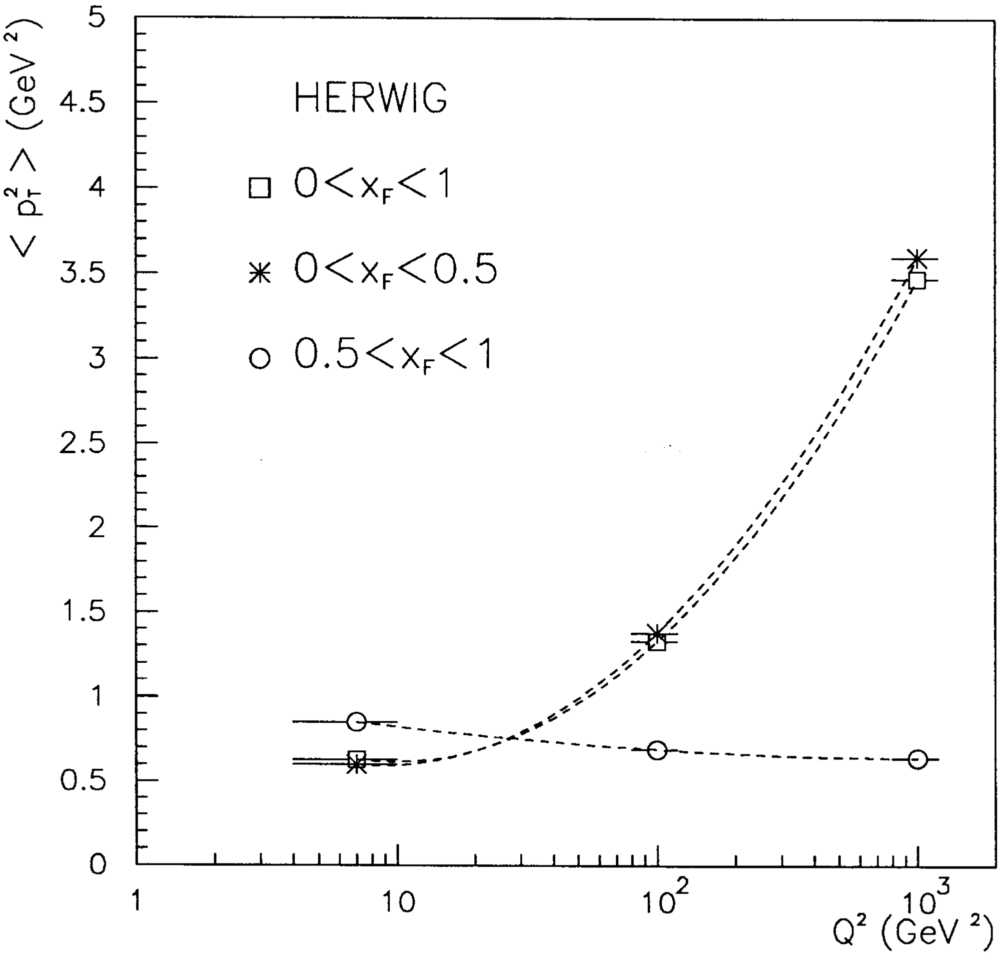
HERWIG
0<x_F<1
0<x_F<0.5
0.5<x_F<1
< p_T^2 > (GeV ²)
Q² (GeV ²)
0
0.5
1
1.5
2
2.5
3
3.5
4
4.5
5
1
10
10^2
10^3

Fig. 8b

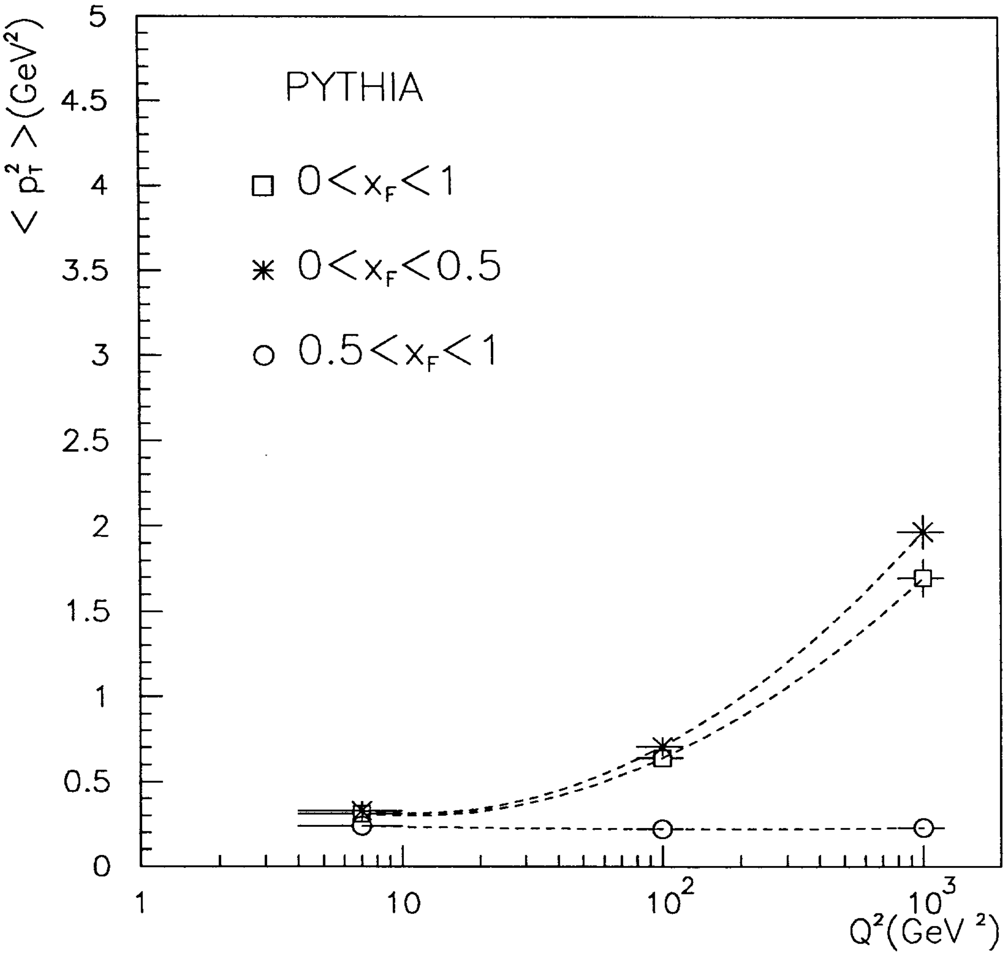

PYTHIA
$0<x_F<1$
$0<x_F<0.5$
$0.5<x_F<1$
$< p_T^2 >(GeV^2)$
$Q^2(GeV^2)$
0
0.5
1
1.5
2
2.5
3
3.5
4
4.5
5
1
10
10^2
10^3

Fig. 8c

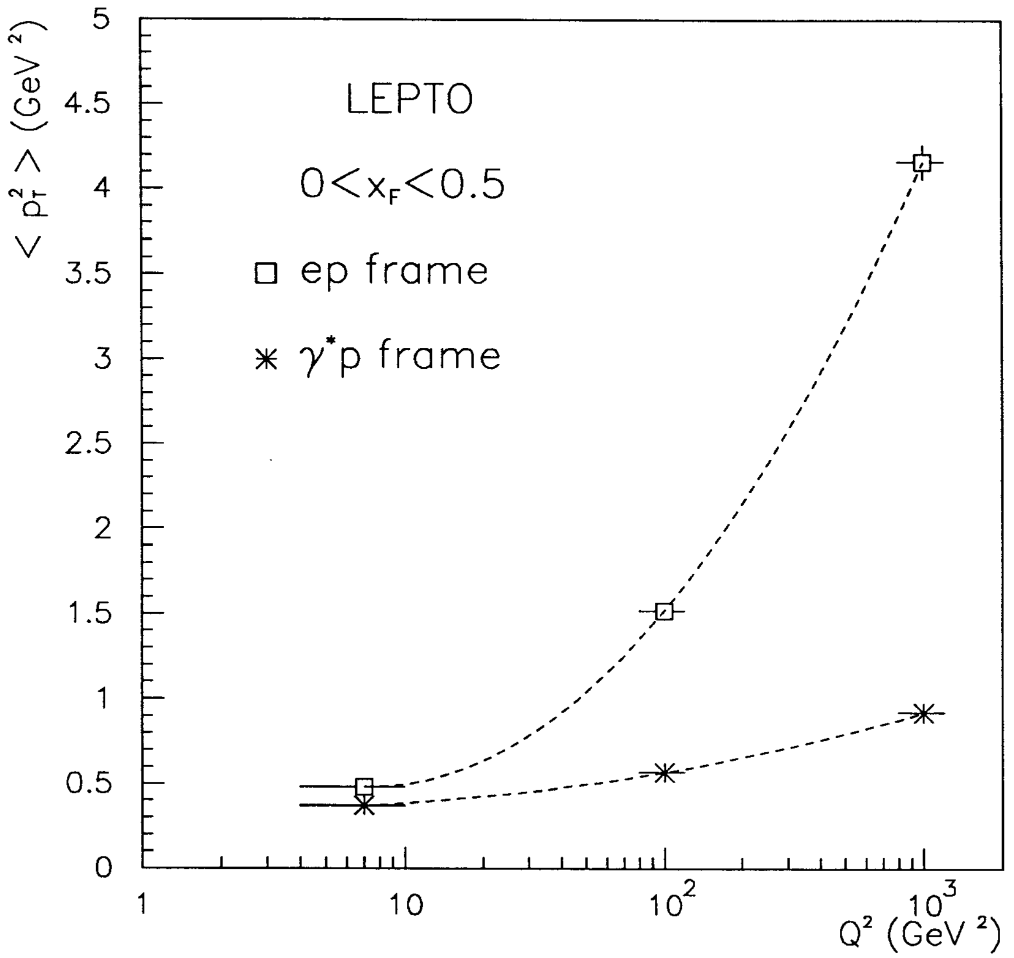
LEPTO
0<x_F<0.5
ep frame
γ*p frame
< p_T^2 > (GeV^2)
Q^2 (GeV^2)
0
0.5
1
1.5
2
2.5
3
3.5
4
4.5
5
1
10
10^2
10^3

Fig. 9a

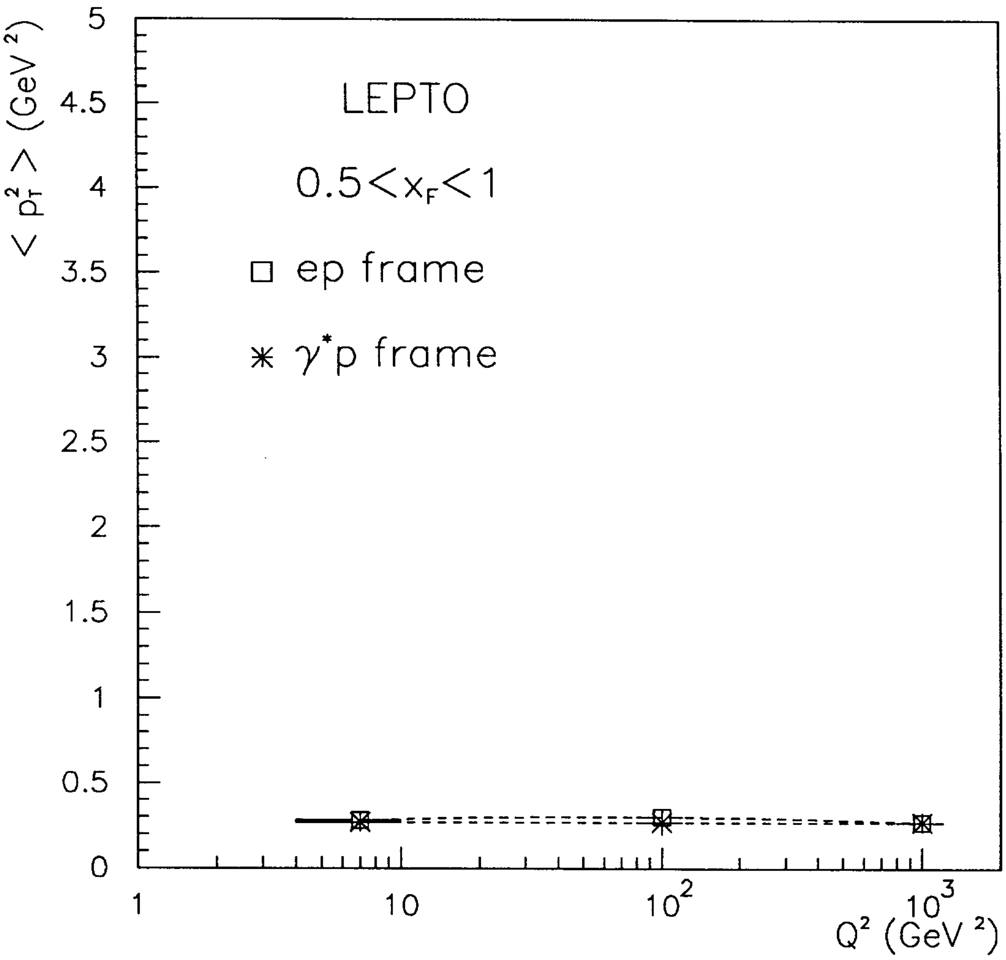

Fig. 9b

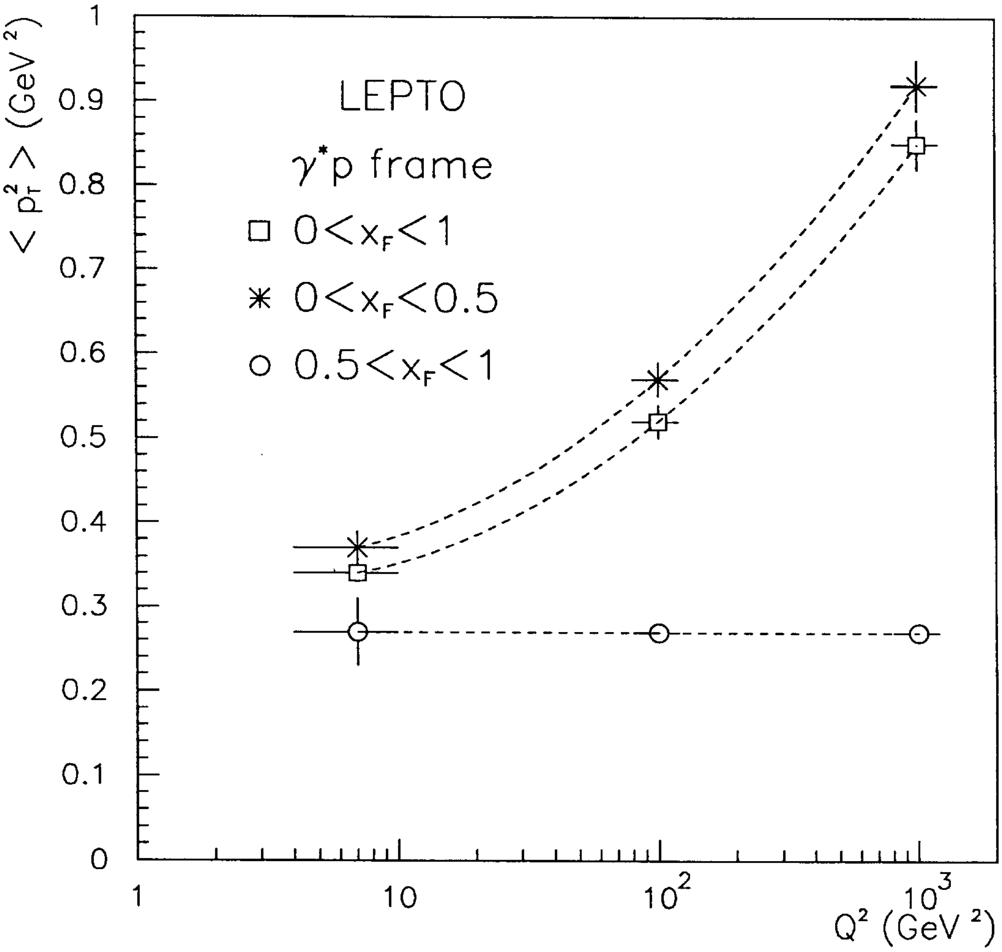
LEPTO
γ^*p frame
$0<x_F<1$
$0<x_F<0.5$
$0.5<x_F<1$
$< p_T^2 >$ (GeV^2)
1
0.9
0.8
0.7
0.6
0.5
0.4
0.3
0.2
0.1
0
1
10
10^2
10^3
Q^2 (GeV^2)

Fig. 10

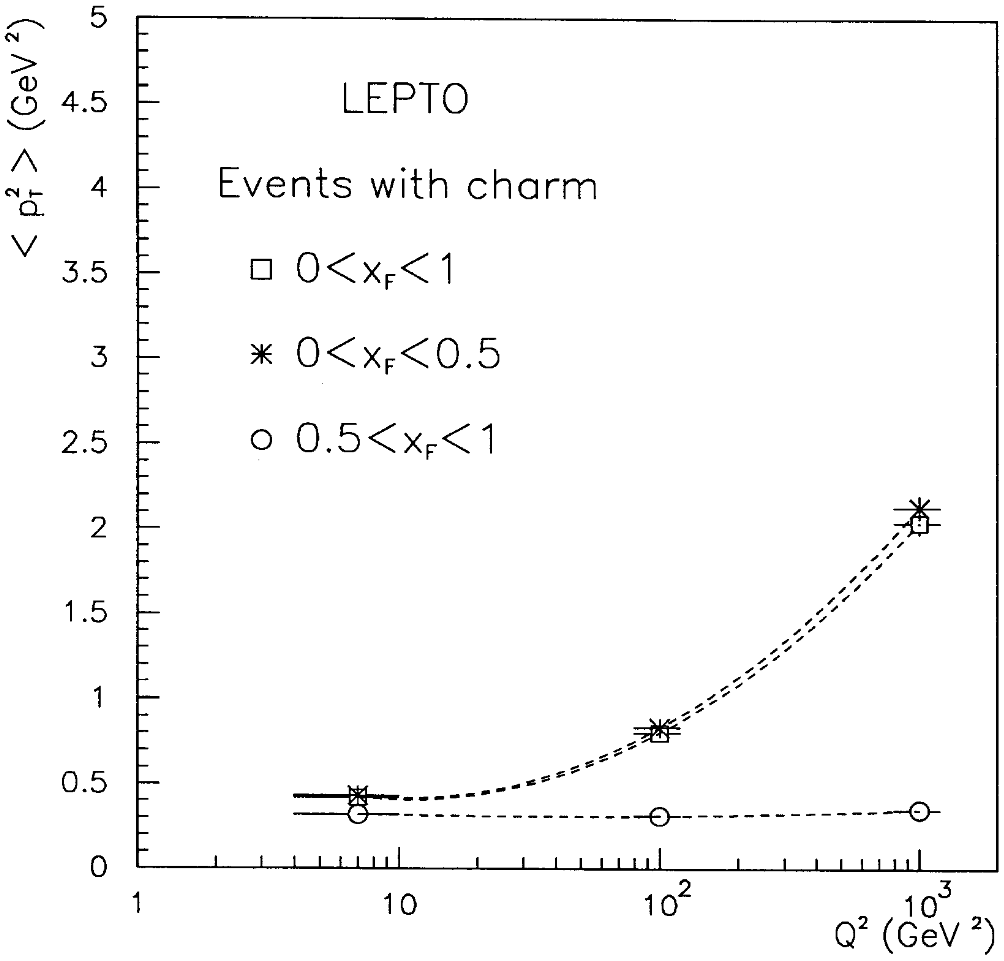
LEPTO
Events with charm
0<x_F<1
0<x_F<0.5
0.5<x_F<1
< p_T^2 > (GeV^2)
Q^2 (GeV^2)
5
4.5
4
3.5
3
2.5
2
1.5
1
0.5
0
1
10
10^2
10^3

Fig. 11a

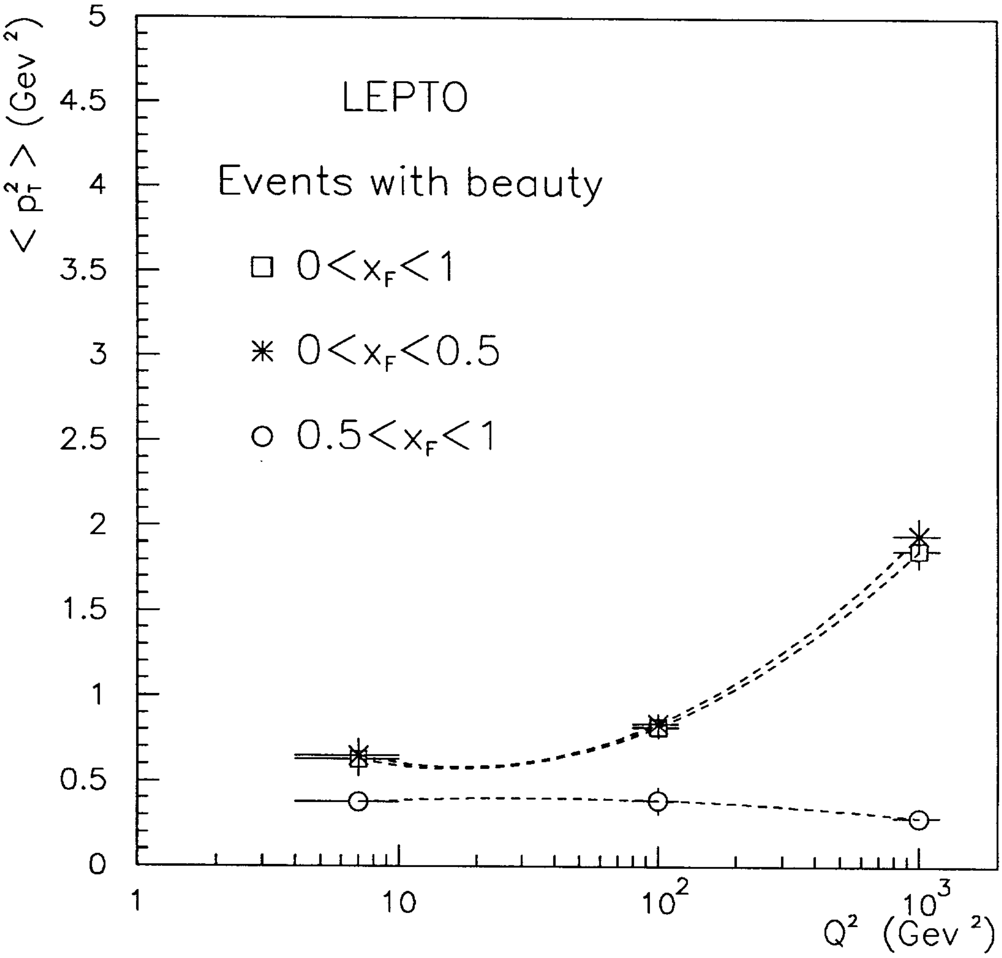
LEPTO
Events with beauty
0<x_F<1
0<x_F<0.5
0.5<x_F<1
< p_T^2 > (Gev ^2)
Q^2 (Gev ^2)
0
0.5
1
1.5
2
2.5
3
3.5
4
4.5
5
1
10
10^2
10^3

Fig. 11b